

Luminescent *cis*-Bis(bipyridyl)ruthenium(II) Complexes with 1,2-Azoylamidino Ligands: Photophysical, Electrochemical Studies, and Photocatalytic Oxidation of Thioethers

Elena Cuéllar, Alberto Diez-Varga, Tomás Torroba, Pablo Domingo-Legarda, José Alemán, Silvia Cabrera, Jose M. Martín-Alvarez, Daniel Miguel, and Fernando Villafañe*

Cite This: *Inorg. Chem.* 2021, 60, 7008–7022

Read Online

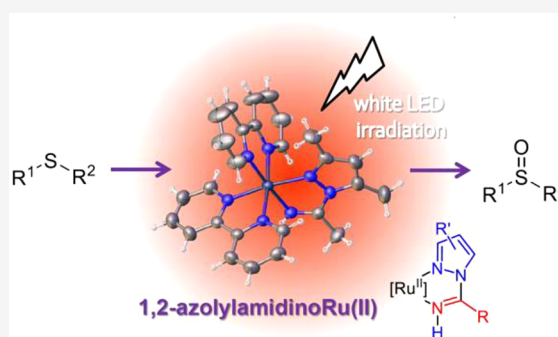
ACCESS |

Metrics & More

Article Recommendations

Supporting Information

ABSTRACT: New 1,2-azoylamidino complexes *cis*-[Ru(bipy)₂(NH=C(R)az* κ^2 N,N)](OTf)₂ (R = Me, Ph; az* = pz, indz, dmpz) are synthesized via chloride abstraction after a subsequent base-catalyzed coupling of a nitrile with the previously coordinated 1,2-azole. The synthetic procedure allows the easy obtainment of complexes having different electronic and steric 1,2-azoylamidino ligands. All of the compounds have been characterized by ¹H, ¹³C, and ¹⁵N NMR and IR spectroscopy and by monocystal X-ray diffraction. Photophysical studies support their phosphorescence, whereas their electrochemistry reveals reversible Ru^{II}/Ru^{III} oxidations between +1.13 and +1.25 V (vs SCE). The complexes have been successfully used as catalysts in the photooxidation of different thioethers, the complex *cis*-[Ru(bipy)₂(NH=C(Me)dmpz κ^2 N,N)]²⁺ showing better catalytic performance in comparison to that of [Ru(bipy)₃]²⁺. Moreover, the significant catalytic performance of the dimethylpyrazolylamidino complex is applied to the preparation of the drug modafinil, which is obtained using ambient oxygen as an oxidant. Finally, mechanistic assays suggest that the oxidation reaction follows a photoredox route via oxygen radical anion formation.



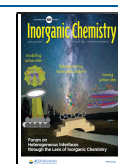
INTRODUCTION

During the last few decades ruthenium complexes with polypyridyl ligands have been luminescent metal complexes studied in great detail. Interest in ruthenium chemistry awoke in the late 1950s and 1960s with two publications: the first report on the luminescent properties of the complex [Ru(bipy)₃]²⁺ (bipy = 2,2'-bipyridyl) by Paris and Brandt¹ and that of the mixed-valence dinuclear complex [(NH₃)₅Ru(μ-pyrazine)Ru(NH₃)₅]⁵⁺ by Creutz and Taube.² The interest in ruthenium complexes with polypyridyl ligands extended broadly during the mid- to late-1970s, after the publication of the dissociation of water into hydrogen and oxygen facilitated by the association of the excited state and the electrochemical behavior of the compound [Ru(bipy)₃]²⁺.³ The initial expectations of this result soon faded, but these promising physicochemical properties encouraged research in other areas of interest,⁴ such as their photocatalytic activity toward the reduction of CO₂⁵ or their function as molecular switches⁶ or cation sensors.⁷ The application of these Ru(II) complexes as photoprobes or photochemical reagents for biomolecules was soon also found.^{8–16} This is related to the discovery of cisplatin and its antitumor effect, which led to the rapid spread of new therapeutic agents based on metals different from platinum.¹⁷

Another interesting aspect of these Ru(II) complexes is their use as visible-light photocatalysts, especially in the activation of organic molecules.^{18–22} Some crucial aspects are, first of all, these complexes absorb visible light to give a stable and long-lived photoexcited state,^{23,24} second, the lifetime of the excited species is adequately long to take part in electron-transfer reactions competing with deactivation processes,²⁵ and finally, their excitation states are very powerful single-electron-transfer reagents.¹⁸ One of the many reactions catalyzed by these types of complexes is the oxidation of sulfides in order to synthesize sulfoxides.^{26–33} The latter have a plethora of applications as chiral auxiliaries in asymmetric synthesis³⁴ and are located in many drugs as well as in natural products.³⁵ From an industrial point of view, the oxidation of sulfides is performed with complexes as catalysts and with peroxides or peracids as oxidants. Nevertheless, this approach presents two main drawbacks: the production of sulfones as byproducts due to

Received: November 16, 2020

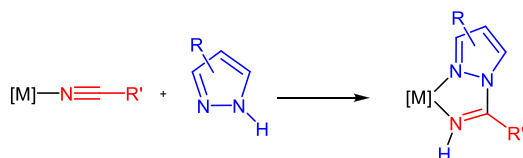
Published: April 27, 2021



overoxidation processes and the difficulties in handling peroxides, which are explosive reagents. In contrast, the oxidation of sulfides, via photocatalysis, using atmospheric O₂ represents a more secure option.

Currently, the search for appropriate *N*-aromatic donor chelate ligands in order to obtain the desired chemical or physical properties of the Ru(II) polypyridyl complexes is one of the main topics of this field. 1,2-Azolyamidino ligands (Scheme 1) have been shown to be an important family of

Scheme 1. Coupling Reaction between a Coordinated Nitrile and a 1,2-Azole to Form a 1,2-Azolyamidino Ligand



ligands, due to not only their electronic delocalization but also the different features of the two nitrogen donor atoms. However, as far as we know, the coordination of such ligands to Ru(II) polypyridyl systems has not been previously reported. The only precedents of bidentate ligands with 1,2-azole moieties also contained 2-pyridyl fragments and were reported several decades ago.^{36,37} The introduction of substituents in the diimine ligands more commonly employed usually requires difficult and often tiresome synthetic methods. The advantage of 1,2-azolyamidino ligands is evident in this aspect: their *in situ* synthesis (Scheme 1) enables the easy production of new bidentate chelates with different electronic and steric properties only by choosing the appropriate nitrile and 1,2-azole, both being readily available. Our previous study on the mechanism describing the coupling of 1,2-azoles and nitriles mediated by complexes broadened the range of synthetic possibilities.³⁸ The acidic hydrogen in the 1,2-azolyamidino ligand is also interesting, since the NH moiety may cause further reactivity. In this regard, the participation of this amino group in intra- or intermolecular noncovalent interactions might lead to the stabilization of a concrete isomer in the first case or to fascinating supramolecular assemblies in the latter case.

Herein we describe the synthesis of new Ru(II) complexes obtained by coordination of the 1,2-azolyamidino ligand to the *cis*-bis(bipyridyl)ruthenium(II) moiety, as well as the spectroscopic, electrochemical, and photophysical behavior of the complexes obtained. The application of the compounds as photocatalysts using O₂ is also evaluated in the oxidation of thioethers.

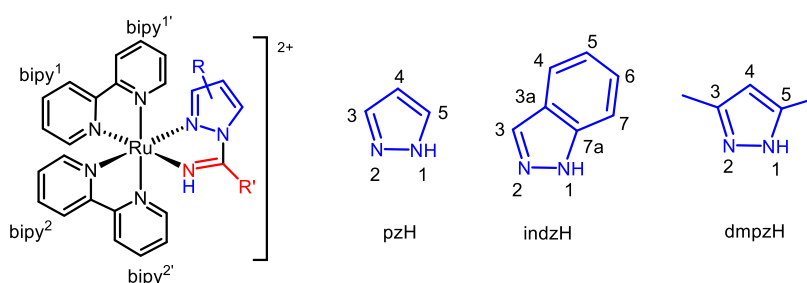


Figure 1. Atomic numbering of bipy, pzH, indzH, and dmpzH for NMR assignment.

EXPERIMENTAL SECTION

General Remarks. All manipulations were carried out under N₂ following conventional Schlenk procedures. Solvents were purified according to standard methods. Complexes **1** and **2** were obtained as previously described by us.³⁹ The rest of the reagents were purchased from the usual commercial suppliers and used as received. Infrared spectra were recorded with a Bruker Tensor 27 FTIR instrument. The abbreviations used to indicate intensity are w = weak, m = medium, s = strong, and vs = very strong. NMR spectra were recorded on a 500 MHz Agilent DD2 or 400 MHz Agilent MR apparatus in the Laboratorio de Técnicas Instrumentales (LTI, Universidad de Valladolid), using (CD₃)₂CO as the solvent at room temperature (rt) unless otherwise indicated. ¹H, ¹³C, and ¹⁵N NMR chemical shifts (δ) are reported in parts per million (ppm) using the residual solvent peak as an internal reference and are referenced to tetramethylsilane (TMS, for ¹H and ¹³C NMR) or to nitromethane (CH₃NO₂, for ¹⁵N NMR). Coupling constants (*J*) are reported in Hz. Abbreviations used to indicate multiplicity are s = singlet, d = doublet, ddd = doublet of doublets of doublets, dt = doublet of triplets, t = triplet, and m = multiplet. The complete assignment (Figure 1) of the ¹H NMR spectra was supported by COSY and TOCSY and NOESY homonuclear ¹H–¹H correlations, whereas the assignment of ¹³C{¹H} and ¹⁵N NMR data was supported by HMBC and HSQC heteronuclear experiments. Elemental analyses were performed on a Thermo Fisher Scientific EA Flash 2000 instrument.

cis-[Ru(bipy)₂(NH=C(Me)pz-κ²N,N)](OTf)₂ (3a**).** AgOTf (0.026 g, 0.1 mmol) was added to a solution of **1a** (0.068 g, 0.1 mmol) in MeCN (5 mL). A 100 μL portion of aqueous 0.02 M NaOH (0.002 mmol) was then added, and the mixture was stirred at rt for 24 h in the absence of light. The reaction mixture was filtered to remove solid AgCl and dried *in vacuo*. The red residue was crystallized in MeCN/Et₂O at –20 °C, giving a red microcrystalline solid, which was decanted, washed with Et₂O (3 × 3 mL approximately), and dried *in vacuo*: yield 0.059 g (72%). In order to obtain a monocrystalline solid, a slight stoichiometric excess of NH₄PF₆ was added to a solution of the complex in acetone, giving [Ru(bipy)₂(NH=C(Me)pz-κ²N,N)](PF₆)₂ as a red monocrystalline solid. ¹H NMR (500 MHz, acetone-*d*₆): δ 11.37 (s, NH, 1 H), 8.90–8.84 (m, H^{6'} bipy¹ and H⁵ pz, 2 H), 8.81–8.74 (m, H^{3'} bipy¹, H³ bipy² and H^{3'} bipy², 3 H), 8.70 (d, *J* = 7.8 Hz, H³ bipy¹, 1 H), 8.29–8.18 (m, H^{4'} bipy² and H^{4'} bipy¹, 2 H), 8.14 (ddd, *J* = 8.2, 7.6, 1.5 Hz, H⁴ bipy², 1 H), 8.12–8.04 (m, H^{6'} bipy², and H⁴ bipy¹, 1 H), 8.01 (ddd, *J* = 5.7, 1.5, 0.8 Hz, H⁶ bipy², 1 H), 7.93 (ddd, *J* = 5.7, 1.4, 0.8 Hz, H⁶ bipy¹, 1 H), 7.74–7.65 (m, H^{5'} bipy¹, H³ pz, and H^{5'} bipy², 3 H), 7.51 (ddd, *J* = 7.5, 5.6, 1.3 Hz, H⁵ bipy², 1 H), 7.45 (ddd, *J* = 7.5, 5.6, 1.3 Hz, H⁵ bipy¹, 1 H), 6.86 (dd, *J* = 3.2, 2.1 Hz, H⁴ pz, 1 H), 3.07 (d, *J* = 1.1 Hz, NH=CCH₃, 3 H). ¹³C NMR (126 MHz, acetone): δ 163.05 (1C, NH=CCH₃), 157.95 (1C, C² bipy¹), 157.63 (1C, C² bipy²), 157.46 (2C, C^{2'} bipy¹ and C^{2'} bipy²), 153.53 (1C, C^{6'} bipy¹), 152.21 (1C, C⁶ bipy¹), 151.87 (1C, C⁶ bipy²), 151.69 (1C, C^{6'} bipy²), 145.45 (1C, C³ pz), 137.70 (1C, C^{4'} bipy²), 137.57 (1C, C^{4'} bipy¹), 137.42 (1C, C⁴ bipy²), 137.32 (1C, C⁴ bipy¹), 134.06 (1C, C⁵ pz), 127.68 (1C, C^{5'} bipy²), 127.50 (1C, C^{5'} bipy¹), 127.07 (1C, C⁵ bipy²), 126.84 (1C, C⁵ bipy¹), 123.92 (1C, C^{3'} bipy¹), 123.89 (1C, C³ bipy²), 123.75 (1C, C^{3'} bipy²), 123.70 (1C, C^{3'} bipy¹), 111.53 (1C, C⁴ pz), 17.94 (1C, NH=CCH₃). IR (solid,

cm⁻¹): 3237 m, 3117 w, 3092 w, 2929 w, 2290 w, 2164 w, 2140 w, 2051 w, 1981 w, 1913 w, 1695 m, 1638 m, 1605 w, 1568 w, 1523 w, 1466 s, 1445 s, 1420 s, 1402 m, 1378 w, 1329 w, 1315 w, 1263 vs, 1222 vs, 1141 vs, 1071 m, 1048 m, 1026 vs, 958 s, 911 m, 850 m, 801 w, 762 vs, 744 s, 429 vs, 681 w, 659 w, 632 vs. Anal. Calcd for C₂₇H₂₃F₆N₇O₆RuS₂: C, 39.51; H, 2.82; N, 11.95; S, 7.81. Found: C, 39.85; H, 2.74; N, 11.84; S, 8.19.

cis-[Ru(bipy)₂(NH=C(Me)indz-κ²N,N)](OTf)₂ (3b). A procedure similar to that for 3a, using 1b (0.072 g, 0.1 mmol) as the starting material, but without addition of the NaOH solution, gave 0.065 g (75%) of 3b as a red microcrystalline solid. ¹H NMR (500 MHz, acetone-*d*₆): δ 10.99 (s, NH, 1 H), 8.90 (d, *J* = 5.6 Hz, H^{6'} bipy¹, 1 H), 8.80 (d, *J* = 8.2 Hz, H^{3'} bipy¹, H³ bipy¹ and H^{3'} bipy², 3 H), 8.73 (d, *J* = 8.2 Hz, H³ bipy², 1 H), 8.37 (d, *J* = 0.8 Hz, H³ indz, 1 H), 8.28–8.21 (m, H^{6'} and H^{4'} bipy², 2 H), 8.23–8.14 (m, H^{4'} bipy¹, H⁴ bipy¹, and H⁷ indz, 3 H), 8.10 (t, *J* = 7.9 Hz, H⁴ bipy², 1 H), 8.06 (d, *J* = 4.9 Hz, H⁶ bipy¹, 1 H), 7.95 (d, *J* = 6.4 Hz, H⁶ bipy², 1 H), 7.84 (d, *J* = 8.1 Hz, H⁴ indz, 1 H), 7.71 (ddd, *J* = 8.5, 7.2, 1.1 Hz, H⁶ indz, 1 H), 7.66 (ddd, *J* = 7.0, 5.6, 1.3 Hz, H^{5'} bipy¹, 1 H), 7.60 (ddd, *J* = 7.0, 5.6, 1.3 Hz, H^{5'} bipy², 1 H), 7.55 (ddd, *J* = 7.0, 5.6, 1.3 Hz, H⁵ bipy¹, 1 H), 7.50–7.42 (m, H⁵ bipy² and H⁵ indz, 2 H), 3.37 (s, NH=CCH₃, 3 H). ¹³C NMR (126 MHz, acetone-*d*₆): δ 163.68 (1C, NH=CCH₃), 157.57 (2C, C² bipy² and C² bipy¹), 157.39 (1C, C^{2'} bipy¹), 157.29 (1C, C^{2'} bipy²), 153.53 (1C, C^{6'} bipy¹), 151.95 (1C, C⁶ bipy²), 151.82 (1C, C⁶ bipy¹), 151.79 (1C, C^{6'} bipy²), 142.87 (1C, C³ indz), 140.03 (1C, C^{7a} indz), 137.73 (1C, C^{4'} bipy²), 137.70 (1C, C^{4'} bipy¹), 137.60 (1C, C⁴ bipy¹), 137.46 (1C, C⁴ bipy²), 130.09 (1C, C⁶ indz), 127.60 (1C, C^{5'} bipy²), 127.49 (1C, C^{5'} bipy¹), 127.20 (1C, C⁵ bipy¹), 126.87 (1C, C⁵ bipy²), 126.64 (1C, C^{3a} indz), 124.72 (1C, C⁵ indz), 124.04 (2C, C³ bipy¹ and C^{3'} bipy¹), 123.79 (1C, C^{3'} bipy²), 123.73 (1C, C³ bipy²), 121.69 (1C, C⁴ indz), 112.16 (1C, C⁷ indz), 20.44 (1C, NH=CCH₃). ¹⁵N NMR (51 MHz, acetone-*d*₆): δ -119.46 (1N, N² indz), -129.11 (1N, N^{1'} bipy¹), -129.88 (1N, N^{1'} bipy²), -130.40 (1N, N¹ bipy¹), -133.12 (1N, N¹ bipy²), -166.05 (1N, N¹ indz), -185.22 (1N, NH). IR (solid, cm⁻¹): 3190 m, 3090 w, 2989 w, 2935 w, 2626 w, 2288 w, 2187 w, 2164 w, 2140 w, 2113 w, 2051 w, 2018 w, 1981 w, 1903 w, 1853 w, 1781 w, 1694 s, 1632 m, 1602 w, 1509 w, 1462 s, 1435 s, 1420 s, 1348 w, 1251 vs, 1224 vs, 1191 s, 1141 vs, 1081 m, 1029 vs, 913 w, 889 m, 858 m, 836 m, 805 w, 770 vs, 749 vs, 730 s, 714 m, 661 w, 632 vs. Anal. Calcd for C₃₁H₂₅F₆N₇O₆RuS₂: C, 42.76; H, 2.89; N, 11.26; S, 7.36. Found: C, 43.01; H, 2.83; N, 11.44; S, 7.80.

cis-[Ru(bipy)₂(NH=C(Me)dmpz-κ²N,N)](OTf)₂ (3c). The same procedure as for 3a, using 1c (0.069 g, 0.1 mmol) as the starting material, gave 0.060 g (71%) of 3c as a red microcrystalline solid. ¹H NMR (500 MHz, acetone-*d*₆): δ 11.13 (s, NH, 1 H), 8.85 (d, *J* = 4.9 Hz, H^{6'} bipy¹, 1 H), 8.82–8.74 (m, H³ bipy¹, H^{3'} bipy¹ and H^{3'} bipy², 3 H), 8.67 (dt, *J* = 8.2, 1.0 Hz, H³ bipy², 1 H), 8.29–8.19 (m, H^{4'} bipy¹ and H^{4'} and H^{6'} bipy², 3 H), 8.13 (td, *J* = 8.2, 1.5 Hz, H⁴ bipy¹, 1 H), 8.09–8.01 (m, H⁴ bipy² and H⁶ bipy¹, 2 H), 7.78 (d, *J* = 4.3 Hz, H⁶ bipy², 1 H), 7.73 (ddd, *J* = 7.6, 5.6, 1.3 Hz, H^{5'} bipy¹, 1 H), 7.69 (ddd, *J* = 7.1, 5.6, 1.3 Hz, H^{5'} bipy², 1 H), 7.51 (ddd, *J* = 7.2, 5.7, 1.3 Hz, H⁵ bipy¹, 1 H), 7.41 (ddd, *J* = 7.0, 5.7, 1.3 Hz, H⁵ bipy², 1 H), 6.44 (s, H⁴ dmpz, 1 H), 3.11 (s, NH=CCH₃, 3 H), 2.81 (s, CH₃⁵ dmpz, 3 H), 1.64 (s, CH₃³ dmpz, 3 H). ¹³C NMR (126 MHz, acetone): δ 164.45 (1C, NH=CCH₃), 157.97 (1C, C² bipy²), 157.53 (1C, C² bipy¹), 157.42 (1C, C^{2'} bipy²), 157.31 (1C, C^{2'} bipy¹), 157.13 (1C, C³ dmpz), 153.01 (1C, C^{6'} bipy¹), 152.18 (1C, C^{6'} bipy²), 151.97 (1C, C⁶ bipy²), 151.65 (1C, C⁶ bipy¹), 146.75 (1C, C⁵ dmpz), 137.46 (2C, C^{4'} bipy¹ and C^{4'} bipy²), 137.32 (2C, C⁴ bipy¹ and C⁴ bipy²), 127.73 (1C, C^{5'} bipy²), 127.52 (1C, C^{5'} bipy¹), 127.39 (1C, C⁵ bipy¹), 126.90 (1C, C⁵ bipy²), 124.19 (1C, C³ bipy¹), 123.98 (1C, C^{3'} bipy¹), 123.77 (1C, C^{3'} bipy²), 123.66 (1C, C³ bipy²), 113.58 (1C, C⁴ dmpz), 20.82 (1C, NH=CCH₃), 13.56 (1C, CH₃⁵ dmpz), 11.49 (1C, CH₃³ dmpz). ¹⁵N NMR (51 MHz, acetone-*d*₆): δ -126.43 (1N, N¹ bipy¹), -127.55 (1N, N^{1'} bipy¹), -129.02 (1N, N^{1'} bipy²), -133.32 (1N, N¹ bipy²), -141.76 (1N, N² dmpz), -151.25 (1N, N¹ dmpz), -177.07 (1N, NH). IR (solid, cm⁻¹): 3229 m, 3114 m, 3086 m, 2994 w, 2637 w, 2288 w, 2164 w, 2146 w, 2112 w, 2050 w, 1981 w, 1921 w, 1732 m, 1633 m, 1606 m, 1573 m, 1468 s, 1446 s,

1415 vs, 1387 w, 1361 m, 1316 w, 1252 vs, 1221 vs, 1151 vs, 1101 m, 1073 w, 1050 m, 1028 vs, 993 m, 962 m, 891 w, 833 w, 809 w, 766 m, 756 vs, 732 s, 684 w, 661 m, 635 vs. Anal. Calcd for C₂₉H₂₇F₆N₇O₆RuS₂: C, 41.04; H, 3.21; N, 11.55; S, 7.55. Found: C, 41.26; H, 3.15; N, 11.87; S, 8.15.

cis-[Ru(bipy)₂(NH=C(Ph)pz-κ²N,N)](OTf)₂ (4a). PhCN (100 μL) was added to a solution of 2a (0.080 g, 0.1 mmol) in Me₂CO (5 mL). A 100 μL portion of an aqueous 0.02 M solution of NaOH (0.002 mmol) was then added, and the mixture was stirred at rt for 24 h. The red solution was crystallized in acetone/Et₂O at -20 °C, giving a red microcrystalline solid, which was decanted, washed with Et₂O (3 × 3 mL approximately), and dried *in vacuo*: yield 0.059 g (67%). ¹H NMR (400 MHz, acetone-*d*₆): δ 11.77 (s, NH, 1 H), 8.95 (d, *J* = 5.3 Hz, H^{6'} bipy¹, 1 H), 8.84–8.76 (m, H^{3'} bipy¹ and H^{3'} bipy², 2 H), 8.72 (m, H³ bipy¹ and H³ bipy², 2 H), 8.65 (d, *J* = 3.4 Hz, H⁵ pz, 1 H), 8.29–8.21 (m, H^{6'} bipy², H^{4'} bipy¹ and H^{4'} bipy², 3 H), 8.16 (td, *J* = 7.8, 1.5 Hz, 1 H), 8.14–8.10 (m, H⁴ bipy¹, 1 H), 8.09–8.03 (m, H⁶ bipy², 1 H), 7.97 (dt, *J* = 7.2, 1.3 Hz, H⁶ bipy¹ and *o*-C₆H₅, 3 H), 7.80 (d, *J* = 2.1 Hz, H³ pz, 1 H), 7.79–7.69 (m, H^{5'} bipy¹, H^{5'} bipy² and *p*-C₆H₅, 3 H), 7.63 (ddd, *J* = 8.8, 6.8, 1.5 Hz, *m*-C₆H₅, 2 H), 7.53 (ddt, *J* = 8.4, 6.9, 2.1 Hz, H⁵ bipy¹, 1 H), 7.46 (ddd, *J* = 7.6, 4.4, 1.5 Hz, H⁵ bipy², 1 H), 6.89 (dd, *J* = 3.4, 2.0 Hz, H⁴ pz, 1 H). ¹³C NMR (101 MHz, acetone): δ 163.85 (1C, NH=CPh), 157.99 (1C, C² bipy¹), 157.55 (1C, C² bipy²), 157.44 (2C, C^{2'} bipy¹ and C^{2'} bipy²), 153.45 (1C, C^{6'} bipy¹), 152.31 (1C, C^{6'} bipy²), 151.90 (1C, C⁶ bipy²), 151.72 (1C, C^{6'} bipy²), 146.03 (1C, C³ pz), 137.95 (1C, C^{4'} bipy²), 137.82 (1C, C^{4'} bipy¹), 137.64 (1C, C⁴ bipy²), 137.47 (1C, C⁴ bipy¹), 135.41 (1C, C⁵ pz), 132.94 (1C, *p*-C₆H₅), 129.38 (2C, *m*-C₆H₅), 129.23 (1C, *ipso*-C₆H₅), 128.92 (2C, *o*-C₆H₅), 127.88 (1C, C⁵ bipy²), 127.69 (1C, C^{5'} bipy¹), 127.17 (1C, C⁵ bipy¹), 126.85 (1C, C⁵ bipy¹), 124.08 (1C, C^{3'} bipy¹), 124.00 (1C, C^{3'} bipy²), 123.81 (1C, C³ bipy²), 123.71 (1C, C³ bipy¹), 112.05 (1C, C⁴ pz). ¹⁵N NMR (51 MHz, acetone-*d*₆): δ -128.17 (1N, N^{1'} bipy¹), -131.19 (1N, N^{1'} bipy²), -131.53 (1N, N¹ bipy²), -134.46 (1N, N¹ bipy¹), -141.51 (1N, N¹ pz), -147.69 (1N, N² pz), -169.98 (1N, NH). IR (solid, cm⁻¹): 3501 w, 3114 m, 3082 m, 2977 w, 2870 w, 2644 w, 2324 w, 2288 w, 2187 w, 2164 w, 2149 w, 2112 w, 2051 w, 2011 w, 1981 w, 1916 w, 1607 m, 1571 w, 1521 w, 1495 w, 1467 m, 1448 s, 1433 s, 1387 m, 1315 w, 1255 vs, 1222 vs, 1147 vs, 1089 s, 1027 vs, 980 m, 895 m, 849 w, 804 w, 763 vs, 731 s, 705 s, 662 w, 634 vs. Anal. Calcd for C₃₂H₂₅F₆N₇O₆RuS₂: C, 43.53; H, 2.86; N, 11.11; S, 7.27. Found: C, 43.73; H, 3.00; N, 10.89; S, 7.11.

cis-[Ru(bipy)₂(NH=C(Ph)indz-κ²N,N)](OTf)₂ (4b). A procedure similar to that for 4a, using 2b (0.085 g, 0.1 mmol) as the starting material, but without addition of the NaOH solution, gave 0.067 g (72%) of 4b as a red microcrystalline solid. ¹H NMR (500 MHz, acetone-*d*₆, 278 K): δ 11.26 (s, NH, 1 H), 9.04 (d, *J* = 6.3 Hz, H^{6'} bipy¹, 1 H), 8.85 (d, *J* = 8.2 Hz, H³ bipy¹ and H^{3'} bipy¹, 2 H), 8.82 (d, *J* = 8.2 Hz, H^{3'} bipy², 1 H), 8.75 (d, *J* = 8.1 Hz, H³ bipy², 1 H), 8.57 (d, *J* = 5.6 Hz, H^{6'} bipy², 1 H), 8.49 (s, H³ indz, 1 H), 8.29 (td, *J* = 8.0, 1.5 Hz, H^{4'} bipy², 1 H), 8.26–8.19 (m, H⁴ bipy¹ and H^{4'} bipy¹, 2 H), 8.17–8.09 (m, H⁶ bipy¹, H⁴ bipy² and *o*-C₆H₅, 3 H), 8.02 (d, *J* = 6.4 Hz, H⁶ bipy², 1 H), 7.85–7.63 (m, H⁴ indz, H^{5'} bipy¹, H^{5'} bipy², *p*-C₆H₅, *m*-C₆H₅ and *o*-C₆H₅, 7 H), 7.60 (ddd, *J* = 7.5, 5.6, 1.3 Hz, H⁵ bipy¹, 1 H), 7.50 (ddd, *J* = 7.3, 5.7, 1.3 Hz, H⁵ bipy², 1 H), 7.45–7.39 (m, H⁵ indz and H⁶ indz, 2 H), 6.66 (s, H⁷ indz, 1 H). ¹H NMR (500 MHz, acetone-*d*₆, 243 K): δ 11.26 (s, NH, 1 H), 9.04 (d, *J* = 6.3 Hz, H^{6'} bipy¹, 1 H), 8.85 (d, *J* = 8.2 Hz, H³ bipy¹ and H^{3'} bipy¹, 2 H), 8.82 (d, *J* = 8.2 Hz, H^{3'} bipy², 1 H), 8.75 (d, *J* = 8.1 Hz, H³ bipy², 1 H), 8.57 (d, *J* = 5.6 Hz, H^{6'} bipy², 1 H), 8.49 (s, H³ indz, 1 H), 8.29 (td, *J* = 8.0, 1.5 Hz, H^{4'} bipy², 1 H), 8.26–8.19 (m, H⁴ bipy¹ and H^{4'} bipy¹, 2 H), 8.17–8.09 (m, H⁶ bipy¹, H⁴ bipy² and *o*-C₆H₅, 3 H), 8.02 (d, *J* = 6.4 Hz, H⁶ bipy², 1 H), 7.85–7.76 (m, H⁴ indz, *o*-C₆H₅, *m*-C₆H₅ and *p*-C₆H₅, 4 H), 7.72 (dddd, *J* = 9.1, 7.3, 5.7, 1.3 Hz, H^{5'} bipy¹ and H^{5'} bipy², 2 H), 7.66 (td, *J* = 7.5, 1.5 Hz, *m*-C₆H₅, 1 H), 7.60 (ddd, *J* = 7.5, 5.6, 1.3 Hz, H⁵ bipy¹, 1 H), 7.50 (ddd, *J* = 7.3, 5.7, 1.3 Hz, H⁵ bipy², 1 H), 7.45–7.39 (m, H⁵ indz and H⁶ indz, 2 H), 6.66 (s, H⁷ indz, 1 H). ¹³C NMR (126 MHz, acetone, 298 K): δ 164.47 (1C, NH=CPh), 157.75 (1C, C² bipy²), 157.50 (1C, C² bipy¹), 157.44 (1C, C^{2'} bipy²), 157.43 (1C, C^{2'} bipy¹), 153.55 (1C,

bipy¹), 123.78 (1C, C³ bipy²), 116.66 (2C, *m*-C₆H₅), 112.24 (1C, C⁴ pz). IR (solid, cm⁻¹): 3322 m, 3085 w, 2862 w, 2324 w, 2163 w, 2141 w, 2113 w, 2050 w, 1981 w, 1658 w, 1606 w, 1530 w, 1465 m, 1423 s, 1243 m, 1161 m, 1126 m, 1048 m, 1028 m, 993 m, 829 vs, 758 s, 740 s, 716 s, 637 m. Anal. Calcd for C₃₂H₂₄F₈N₇O₆RuS₂: C, 42.67 H, 2.69; N, 10.89; S, 7.12. Found: C, 42.88; H, 2.98; N, 10.52; S, 7.35.

General Procedure for the Oxidation of Sulfides. A glass vial was loaded with the corresponding sulfide 7a–g (0.2 mmol), and complex 3c (0.002 mmol, 1 mol %). Then, 2.0 mL of absolute ethanol was added, and the reaction mixture was stirred without exclusion of air under irradiation of a white LED system (see the Supporting Information). After 1 h of stirring at rt, the crude reaction mixture was filtered over a plug of Celite/silica gel to afford the corresponding pure sulfoxide 8a–g.

Methyl 4-Methylphenyl Sulfoxide (8a).²⁶ Colorless oil (29.5 mg, 98% yield). ¹H NMR (300 MHz, CDCl₃): δ 7.51 (d, *J* = 8.3 Hz, H² and H⁶ Ar, 2H), 7.30 (d, *J* = 8.3 Hz, H³ and H⁵ Ar, 2H), 2.67 (s, CH₃-SO, 3H), 2.38 (s, CH₃-Ar, 3H).

Benzyl Phenyl Sulfoxide (8b).²⁶ Beige solid (39.9 mg, 92% yield). ¹H NMR (300 MHz, CDCl₃): δ 7.39–7.29 (m, Ph-SO, 5H), 7.22–7.15 (m, Ph of Bn, 3H), 6.92–6.89 (m, Ph of Bn, 2H), 4.02 (d, *J* = 12.6 Hz, CH₂, 1H), 3.92 (d, *J* = 12.6 Hz, CH₂, 1H).

Allyl Phenyl Sulfoxide (8c).²⁶ Colorless oil (29.7 mg, 90% yield). ¹H NMR (300 MHz, CDCl₃): δ 7.61–7.58 (m, H² and H⁶ Ar, 2H), 7.51–7.49 (m, H³, H⁵ and H⁴ Ar, 3H), 5.71–5.57 (m, CH=, 1H), 5.33 (d, *J* = 9.8 Hz, CH₂=, 1H), 5.19 (d, *J* = 16.0 Hz, CH₂=, 1H), 3.46–3.60 (m, CH₂, 2H).

Dibutyl Sulfoxide (8d).²⁶ Colorless oil (24.4 mg, 75% yield). ¹H NMR (300 MHz, CDCl₃): δ 2.75–2.55 (m, CH₂-SO, 4H), 1.85–1.65 (m, CH₂-CH₂-SO, 4H), 1.63–1.32 (m, CH₂-CH₂-CH₂-SO, 4H), 0.97 (t, *J* = 7.3 Hz, CH₃, 6H).

(tert-Butyl)methylsulfoxide (8e).²⁶ Colorless oil (18.6 mg, 78% yield). ¹H NMR (300 MHz, CDCl₃): δ 2.36 (s, CH₃-SO, 3H), 1.24 (s, *t*Bu, 9H).

2-[(Diphenylmethyl)sulfinyl]acetamide, Modafinil (8f).⁴⁰

The crude mixture was purified by flash chromatography (dichloromethane/methanol 10/1 as eluent) to afford 8f as a white solid (45.6 mg, 79% yield). ¹H NMR (300 MHz, CDCl₃): δ 7.50 (dd, *J* = 9.1, 3.0 Hz, H⁴ Ph, 2H), 7.43–7.36 (m, H², H⁶, H³, and H⁵ Ph, 8H), 7.03 (br s, NH₂, 1H), 5.55 (br s, NH₂, 1H), 5.10 (s, Ph₂CH, 1H), 3.49 (d, CH₂, *J* = 14.9 Hz, 1H), 3.09 (d, CH₂, *J* = 14.9 Hz, 1H).

Photophysical Experiments. The solvents used for the spectroscopic studies were of spectroscopic grade and were used as received. Fluorescence and ultraviolet–visible (UV–vis) spectra were recorded in optically dilute solutions (from 10⁻⁵ to 5 × 10⁻⁵ M), at rt with a quartz cuvette (1 cm × 1 cm), using Hitachi U-3900 and F-7000 fluorescence spectrophotometers, respectively. Fluorescence decay lifetimes were determined in deaerated solvents, using a time-correlated single photon counting instrument (FLS980 Series, Edinburgh instruments) with a 405 nm pulsed LED (Edinburgh instruments, EPL-510) light source having a 50–500 ns pulse. In each solvent the absolute fluorescence quantum yields were obtained using an Edinburgh FLS980 Series instrument with an integrating sphere accessory, using the solvent as a reference. χ^2 is a statistical parameter that accounts for the quality of fit between the model exponential decays and the observed (ideal value = 1). The FAST software package (Edinburgh Instruments) was used to obtain tail fits and numerical deconvolution.

Electrochemical Experiments. Electrochemical experiments were performed in a three-electrode cell with one cavity, using a platinum-disk working electrode (ϕ = 3 mm), a platinum-wire counter electrode (ϕ = 0.5 mm), and a saturated calomel electrode (SCE) reference electrode in acetonitrile. All of the potentials given are referenced to the SCE electrode. The redox properties of all the complexes were studied with cyclic voltammetry (CV) at different scan rates in a 0.1 M solution (nBu₄N)(PF₆) (TBAH) in MeCN, and their redox potentials are also referenced to the SCE electrode.

Crystal Structure Determination for Compounds 3a–c and 4a–c. Crystals were grown by prolonged diffusion of Et₂O into concentrated solutions of the compounds in acetonitrile (for 3a–c) or

acetone (for 4a–c) at –20 °C. All crystallographic details can be found in the CIF files. A crystal was adhered to a glass fiber and fixed to an Agilent SuperNova diffractometer fitted with an Atlas CCD detector. The crystals were maintained at 293(2) K during data collection. The structures were solved using Olex2,⁴¹ with the ShelXT⁴² structure solution program. The structures were then refined with the ShelXL⁴³ refinement package using least-squares minimization. All non-hydrogen atoms were refined anisotropically, whereas hydrogen atoms were fixed in calculated positions and refined with a common thermal parameter as riding atoms. All graphics were made with Olex2, and distances and angles of hydrogen bonds were calculated with PARST^{44,45} (normalized values).^{46,47}

RESULTS AND DISCUSSION

Syntheses and Characterization of the Complexes.

Complexes with varied substituents were obtained in order to

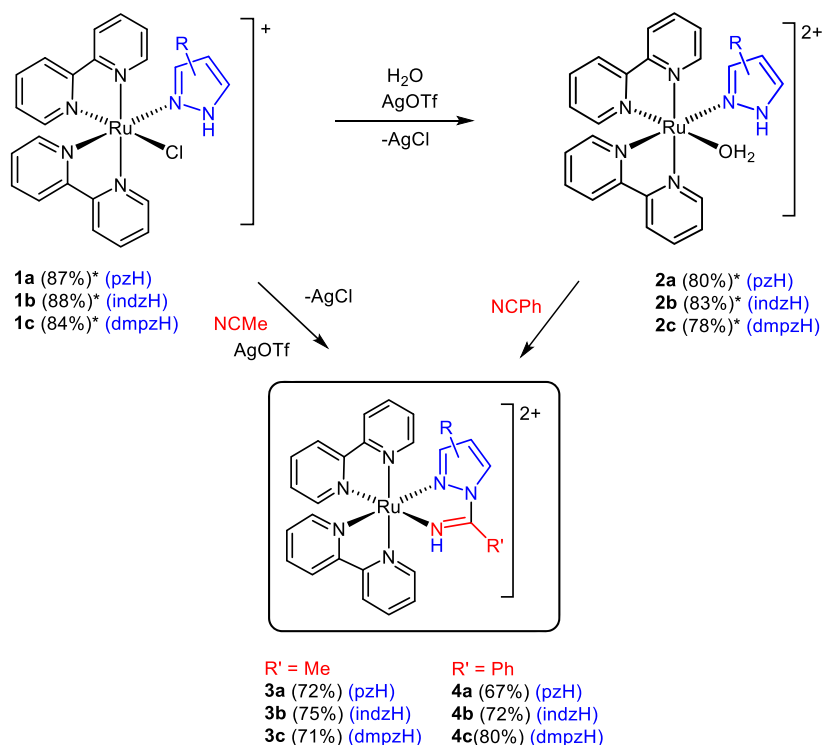
Table 1. Complexes Used in This Study

	pzH	indzH	dmpzH	ref
<i>cis</i> -[Ru(bipy) ₂ Cl(az*H)]OTf	1a	1b	1c	39
<i>cis</i> -[Ru(bipy) ₂ (H ₂ O)(az*H)](OTf) ₂	2a	2b	2c	39
<i>cis</i> -[Ru(bipy) ₂ (NH=C(Me)az*-κ ² N,N)](OTf) ₂	3a	3b	3c	this work
<i>cis</i> -[Ru(bipy) ₂ (NH=C(Ph)az*-κ ² N,N)](OTf) ₂	4a	4b	4c	this work

confirm the synthetic method, as well as to determine the effect of the substituents on the properties of the 1,2-azolylamidino complexes obtained. The 1,2-azolylamidino ligands are the result of the coupling of pyrazole (pzH), indazole (indzH), or 3,5-dimethylpyrazole (dmpzH) with either acetonitrile (MeCN) or benzonitrile (PhCN). All of the complexes described in this work are collected in Table 1 and Scheme 2. In addition to the 1,2-azolylamidino complexes, Table 1 and Scheme 2 include the mixed 1,2-azole–chlorido complexes *cis*-[Ru(bipy)₂Cl(az*H)]OTf (1) and the 1,2-azole–aquo complexes *cis*-[Ru(bipy)₂(H₂O)(az*H)](OTf)₂ (2) previously reported by us³⁹ and used in this work as starting materials.

Chlorido–1,2-azole complexes 1 lead to 1,2-azolylamidino complexes 3, after the chlorido ligand is removed with silver triflate in the presence of MeCN. The 1,2-azolylamidino complexes derived from PhCN are better obtained after removal of the chlorido ligand from 1 in the presence of H₂O to generate the aquo complexes 2,³⁹ which lead to the 1,2-azolylamidino complexes 4 after addition of PhCN. A catalytic amount of NaOH(aq) was added in order to obtain the 1,2-azolylamidino complexes with pz (4a) and dmpz (4c), whereas no base was needed in order to obtain the indazolylamidino complex (4b). This fact is in agreement with the higher acidity of indzH in comparison to pzH or dmpzH.³⁸ The 1,2-azolylamidino complexes with PhCN (4) can also be obtained from the chlorido–1,2-azole precursors 1, by adding PhCN instead of MeCN. However, this route gives lower yields.

Complexes 3 and 4 were all characterized by single-crystal X-ray diffractometry (Figure 2). The distances and angles (CCDC 2044577–2044582) are analogous to those found in other 1,2-azolylamidino ruthenium(II) complexes.^{48–52} In complexes 3b,c and 4a–c, the *N*-bound hydrogens of the 1,2-azolylamidino ligands are involved in hydrogen bonding with an oxygen atom of a OTf⁻ anion. The distances and angles detected for 3b (H(7)⋯O(2) 1.99(6) Å, N(7)⋯O(2) 2.973(1) Å, N(7)–H(7)⋯O(2) 159.6(3)°, 3c (H(7)⋯O(3) 1.92(2) Å, N(7)⋯O(3) 2.842(17) Å, N(7)–H(7)⋯O(3)

Scheme 2. Synthesis of the New 1,2-Azolyamidino Complexes^a

^aYields are given in parentheses; those with an asterisk are reported in ref 39.

149.7(5)°, **4a** (H(7)⋯O(4) 1.89(2) Å, N(7)⋯O(4) 2.831(19) Å, N(7)–H(7)⋯O(4) 150.6(6)°), **4b** (H(7)⋯O(4) 2.032(4) Å, N(7)⋯O(4) 2.821(6) Å, N(7)–H(7)⋯O(4) 149.8(3)°), and **4c** (H(7)⋯O(3) 2.00(9) Å, N(7)⋯O(3) 2.941(9) Å, N(7)–H(7)⋯O(3) 151(8)°) may be considered as “moderate” hydrogen bonds.^{53,54}

The spectroscopic and analytical data of 1,2-azolyamidino complexes **3** and **4** are collected in the [Experimental Section](#) and sustain the proposed geometries. All the ¹H NMR and ¹³C NMR spectra are displayed in the Supporting Information ([Figures S1–S16](#)). Their ¹H, ¹³C, and ¹⁵N NMR spectra show the expected signals. The hydrogen atoms of the phenyl groups in benzonitrile-derived complexes **4b,c** show broad signals in the ¹H NMR and ¹³C NMR spectra at room temperature, which may be explained by considering the slow rotation of the phenyl group. *ortho* and *meta* protons and carbons both become respectively inequivalent due to this slow motion. Spectra recorded at low temperatures gave the expected pattern with sharp signals ([Figures S17 and S18](#)). On the other hand, the NMR spectra of **4a** (where the substituent is pz, smaller than indz and dmpz) display well-defined signals where each *ortho* and each *meta* proton and carbon are equivalents at rt, which indicates that the phenyl group in the pyrazolamidino ligand freely rotates in this complex.

Photophysical Studies. The absorption and emission spectral data for all of the complexes herein reported are collected in [Tables 2 and 3](#). The data for the previously described complexes **1**³⁹ are also included in both tables for comparison purposes. The absorption and emission spectra ([Figure 3](#)) and the wavelength maxima observed at 298 K in different deaerated solvents are summarized in [Figure S19](#) in the Supporting Information. The spectra of complexes **3** and **4** show absorption patterns analogous to those previously

described for similar complexes.^{55–64} In the 250–300 nm region all of the 1,2-azolyamidino complexes exhibit intense absorption bands that may be ascribed to $\pi(L) \rightarrow \pi^*(L)$ intraligand transitions (IL), whereas the broad lower energy bands above 300 nm correspond to $d\pi(\text{Ru}) \rightarrow \pi^*(L)$ metal to ligand charge transfer bands (MLCT). The low-energy bands of all the complexes are blue-shifted when the chlorido–1,2-azole ligands in **1** are substituted by a 1,2-azolyamidino ligand, and these blue shifts are due to electronic effects caused by the substitution of the electron-donating, anionic chlorido ligand by the σ -donating, neutral amidino ligand. A similar behavior was observed for complexes **1** when the chlorido ligand was replaced by an aquo ligand to generate complexes **2**.³⁹ The MLCT band can be easily shifted or tuned depending on the 1,2-azolyamidino substituents, as can be easily concluded from the values collected in [Table 2](#). For example, a comparison of the lower energy bands between complexes derived from the same nitrile leads to the same sequence: indz (**c**) > pz (**a**) > dmpz (**b**) for both complexes **3** (obtained from MeCN) and **4** (obtained from PhCN).

The emission spectra of all the 1,2-azolyamidino complexes display one unstructured broad band in the 610–650 nm region that is solvent-dependent (shifts of ca. 20 nm for all the complexes). The intensities exhibit a severe increase in deaerated solutions in comparison to those prepared without exclusion of air, with no variation in the emission maxima ([Figure S20](#)). These results, as well as the luminescent emission lifetimes (see below), are typical of ³MLCT phosphorescent emissions.^{65,66}

As can be observed in [Table 2](#) and [Figure 3](#), complex **4a** displays an unexpected behavior. In addition to the expected maximum at 613–646 nm, characteristic of Ru(II) polypyridyl complexes,^{55–58} a second emission is detected at 476 nm. This

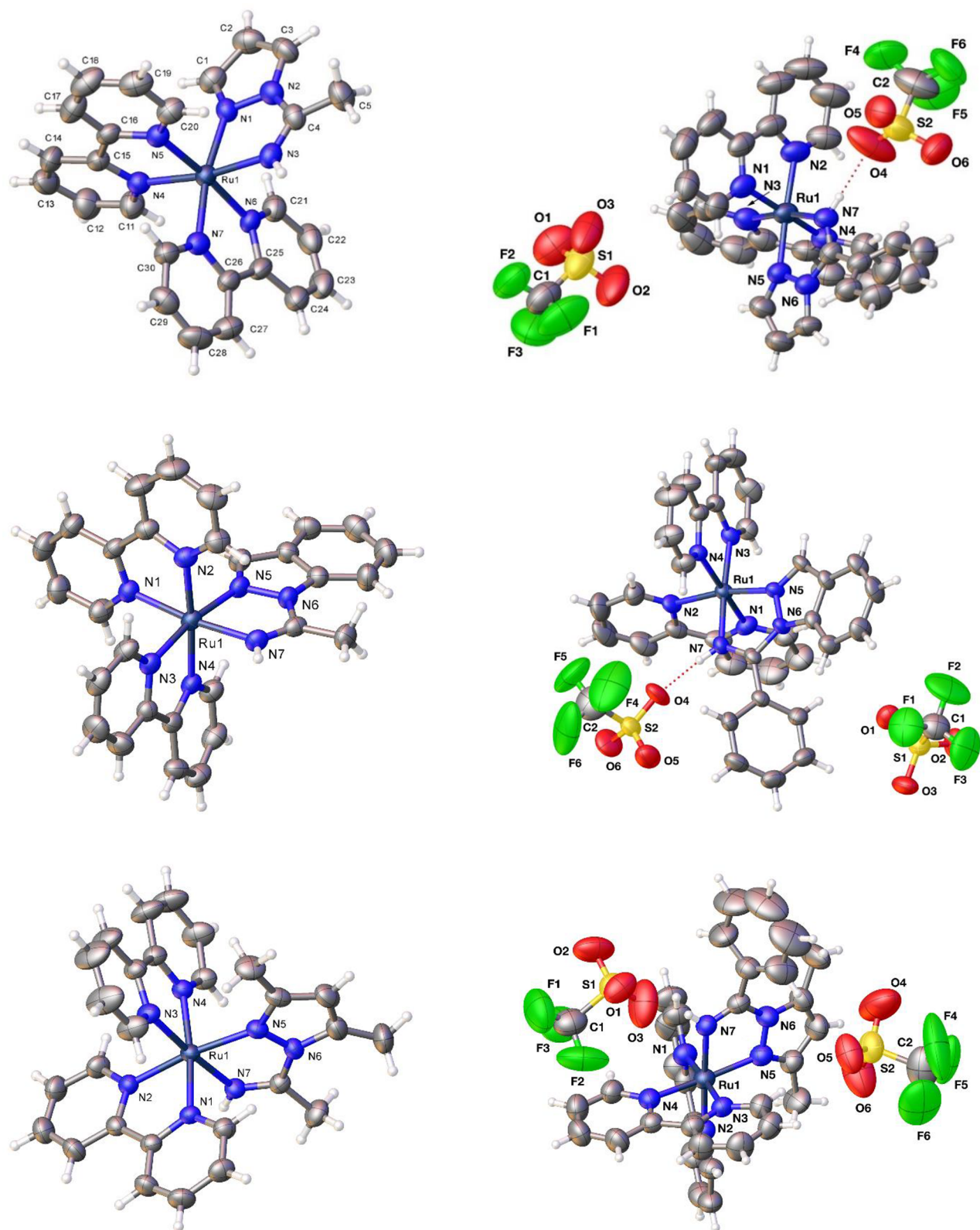


Figure 2. Perspective views of 3a–3c (left from top to bottom, anions not shown) and 4a–c (right from top to bottom, showing triflate anions) showing the atom numbering. Thermal ellipsoids are drawn at 50% probability.

anomalous emission is also detected in THF and acetone solutions (Figure S19). In fact, the emission band at 476 nm is more intense than that at 612 nm in acetone (Figure S19). We have also observed how the intensity of this emission band at

476 nm increases, whereas that at 622 nm decreases, when a solution of 4a in MeCN is irradiated with white light (Figure S21). First, we tried to determine whether this anomalous emission band might be related to electronic effects. The

Table 2. Absorption and Emission Data of Complexes 1 and 3–6 in MeCN

compd	absorption λ (nm) (ϵ (10^{-3} M $^{-1}$ cm $^{-1}$))	emission λ_{em} (nm) ($\lambda_{excit} = 420$ nm)	ref
1a	237 (19.9), 287 (49.5), 341 (7.30), 477 (7.30)	625	39
1b	236 (24.1), 287 (54.9), 338 (8.10), 476 (8.30)	646	39
1c	236 (23.5), 287 (55.8), 341 (8.60), 473 (8.50)	640	39
3a	237 (23.3), 281 (56.4), 365 (7.27), 442 (9.51)	622	this work
3b	232 (40.1), 280 (85.8), 373 (15.6), 410 (17.8)	621	this work
3c	237 (27.3), 283 (61.4), 343 (9.65), 358 (9.55), 456 (10.4)	639	this work
4a	222 (32.0), 237 (31.3), 282 (47.9), 380 (6.88), 431 (9.26)	476, 622	this work
4b	237 (31.0), 281 (64.7), 379 (2.84), 415 (13.6)	629	this work
4c	238 (29.8), 283 (58.7), 338 (7.27), 375 (7.87), 420 (11.1), 445 (11.3)	640	this work
5	235 (31.3), 282 (62.3), 368 (7.58), 441 (11.4)	615	this work
6	238 (28.2), 282 (60.7), 367 (7.16), 446 (10.8)	614	this work

pyrazolylamidino ligand in **4a** is the result of coupling pzH and PhCN. The donor properties of the pyrazolyl moiety are between those of the more electron withdrawing indazolyl (in **4b**) and the more electron donating dimethylpyrazolyl (in **4c**). This sequence is supported by the CO stretching absorptions of *fac*-Re(CO)₃ complexes^{38,67,68} and by the acidity of free 1,2-azoles, experimentally determined.^{69,70} Therefore, a consideration that the anomaly of this complex comes from the pyrazolyl fragment of the bidentate ligand would be difficult to accept. Thus, we turned our attention to the nitrile fragment. The PhCN used to form the 1,2-azolylamidino ligands in complexes **4** is less donating in comparison to the MeCN used to obtain complexes **3**. In order to study whether the electronic effects of the phenyl group affects the anomalous photo-physical properties of **4a**, structurally similar complexes containing a donor group (methyl) or an acceptor group (F) in the para position of the phenyl group were synthesized (the NH=C(*p*-Tol)pz- κ^2 N,N ligand in **5**, and the NH=C(*p*-FC₆H₄)pz- κ^2 N,N ligand in **6**). However, the emission spectra of complexes **5** and **6** (Table 2 and Figure 3) are again similar to those of the complexes described herein, except for **4a**. Therefore, the electronic parameters do not provide an

explanation for the anomalous emission band of **4a**. The emission spectra at 77 K (Figure S22) and in the solid state (Figure S23) were also recorded after suggestions by the reviewers, but they do not provide additional information. We have tried to carry out theoretical calculations to explain this anomaly, but unfortunately all of our attempts have failed so far. Finally, it should be pointed out that dissociation of the 1,2-azolylamidino ligand is not possible, since we have previously described how decoordination of the 1,2-azolylamidino ligands leads to reversal of the coupling reaction of the 1,2-azole and the nitrile, giving again the 1,2-azole–nitrile mixed precursor.³⁸ In this case, prolonged heating at 40 °C (4 h) or irradiation (6 h) of **4a** in (CD₃)₂CO afforded mainly an unmodified product and only negligible amounts of the corresponding aquo and acetone complexes, *cis*-[Ru-(bipy)₂(L)(pzH)](OTf)₂ (L = H₂O (**2a**), (CD₃)₂CO). Therefore, this band cannot be due to a decomposition product.

Since the solvent does not influence the quantum yields or the luminescent emission lifetimes, these properties have been measured in different solvents, subjected to the solubilities of the complexes (Table 3). Both quantum yields and luminescent emission lifetimes are similar to those described for other ruthenium complexes.^{58,71,72} The data of dimethylpyrazolylamidino complex **3c** are remarkable, as they present the highest quantum yield and also the highest luminescence emission lifetime among all the complexes described herein. These results also agree with the higher activity attained by this complex toward the photocatalytic oxidation of thioethers, in comparison to the rest, as detailed below. The comparison among the quantum yields of pyrazolylamidino complexes leads to significant variations (0.017 and 0.041 for **4a** and **3a**, respectively, vs 0.014 for **1a**). When dimethylpyrazolyl complexes are considered, the quantum yield of **3c** (0.061) is also significantly higher than that of the dmpzH complex **1c** (0.0092). Compound **4a** shows a lower lifetime (10.9 ns) and, concomitantly, higher k_r and k_{nr} values (156×10^{-4} and 9020×10^{-4} s $^{-1}$, respectively), which might point to ligand-based luminescence.

Electrochemical Studies. The redox properties of complexes **1** have been previously described.^{73,74} However, for **1a,c** the reduction waves were not showed, for this reason we have reported them again. Moreover, herein we report the electrochemistry of the 1,2-azolylamidino complexes **3** and **4**.

Cyclic voltammograms of **3** and **4** in MeCN exhibit reversible Ru^{II}/Ru^{III} oxidations between +1.13 and +1.25 V

Table 3. Emission Data of Complexes in Different Solvents

compd	solvent	emission					ref
		$10^{-2}\Phi$	τ (ns)	χ^2	k_r (10^4 s $^{-1}$)	k_{nr} (10^4 s $^{-1}$)	
1a	THF	1.4	46.1	1.01	30.6	2140	39
1b	MeCN	0.15	42.1	1.30	3.56	2370	39
1c	MeCN	0.92	178	1.18	5.15	555	39
3a	THF	4.1	50.1	1.15	82.4	1910	this work
3b	THF	0.45	72.0	1.16	6.25	1380	this work
3c	THF	6.1	304	0.99	20.0	309	this work
4a	MeCN	1.7	10.9	1.09	156	9020	this work
4b	THF	0.28	78.1	1.31	3.59	1280	this work
4c	MeCN	0.16	195	1.01	0.821	512	this work
5	H ₂ O	0.50	22.9	1.01	21.8	4350	this work
6	H ₂ O	0.41	22.8	1.03	18.0	4370	this work

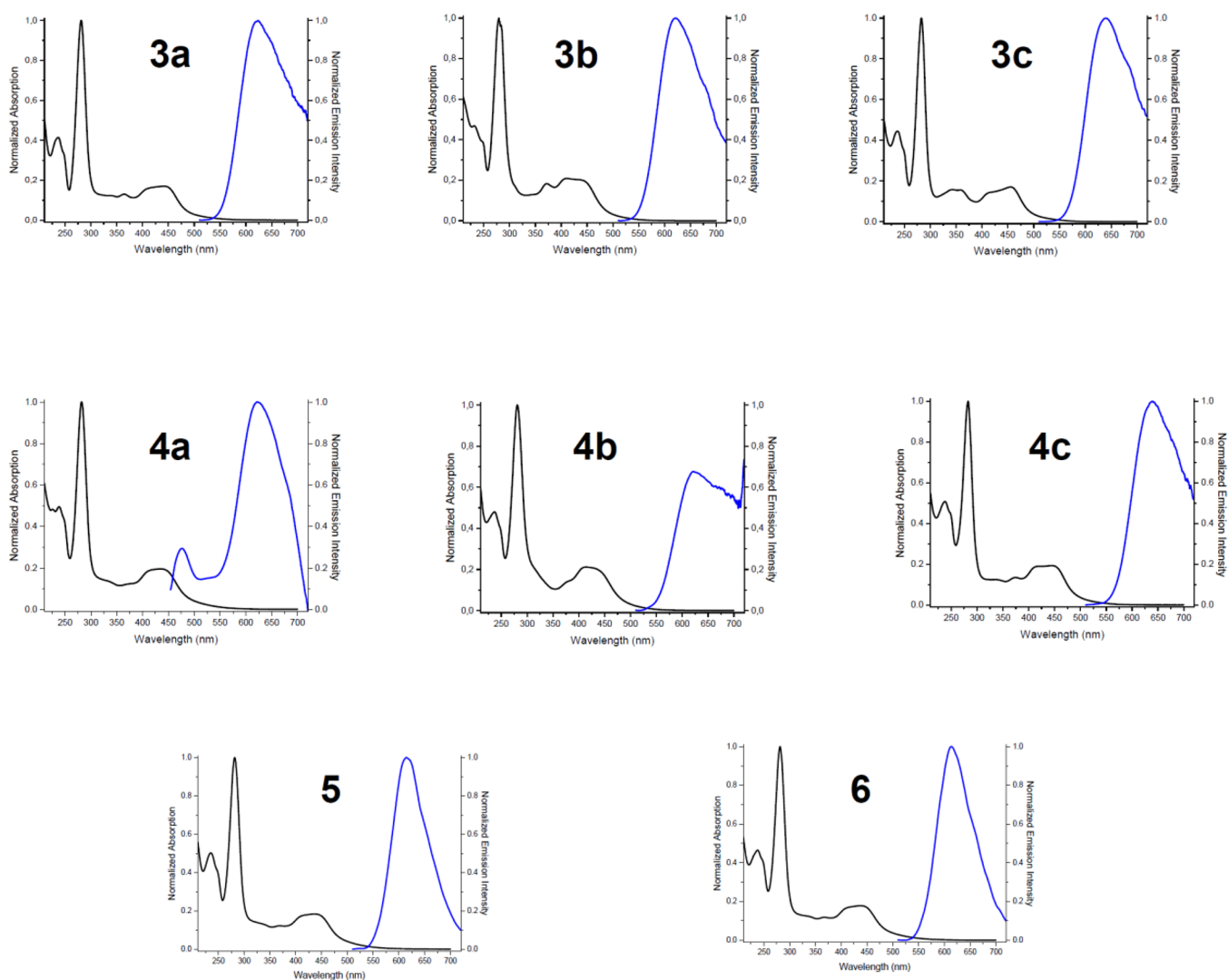


Figure 3. Normalized UV/vis absorption (black) and emission (blue, $\lambda_{\text{ex}} = 420$ nm) spectra, in deaerated solvents in optically dilute MeCN solutions at 298 K.

Table 4. Summary of Ground- and Excited-State Redox Potentials of Complexes 1, 3, and 4

complex	redox potential, $E_{1/2}$ (vs SCE) ^a				
	E_{ox} (V)	E_{red} (V)	E_{0-0} (eV) ^b	E_{ox}^* (V) ^c	E_{red}^* (V) ^c
1a	0.79	-1.52			
1b	0.83	-1.60			
1c	0.78	-1.62			
3a	1.20	-1.43, -1.60	2.27	-1.07	0.84
3b	1.19	-1.42, -1.58	2.28	-1.09	0.86
3c	1.25	-1.49	2.22	-0.97	0.73
4a	1.13	-1.46, -1.66			
4b	1.24	-1.46, -1.65			
4c	1.18	-1.58, -1.68			

^aThe electrochemical data were obtained for acetonitrile solutions; $E_{1/2}$ values were referenced vs SCE, and the scan rate was 100 mV/s.

^bSinglet state energy (E_{0-0}) determined from the intersection of the normalized absorbance and emission spectra and converted into eV.

^cExcited-state redox potentials estimated using the equation $E_{\text{ox}}^* = E_{\text{ox}} - E_{0-0}$ or $E_{\text{red}}^* = E_{\text{red}} + E_{0-0}$.

(vs SCE) (see Table 4 and complete data in the Supporting Information). These values are slightly lower than that found for $[\text{Ru}(\text{bipy})_3]^{2+}$ (+1.29 V in MeCN)⁷⁵ and ca. 0.3–0.5 V higher than those for the chlorido-1,2-azole complexes **1** (+0.78 to +0.83 V). This shift is in agreement with the replacement of the anionic, electron-donating chlorido ligand by the neutral, π -accepting amidino moiety. As expected, this positive variation in the potential is even higher in comparison with the potential of the *cis*- $[\text{Ru}(\text{bipy})_2\text{Cl}_2]$ complex.^{73,74}

Cyclic scans at different scan rates (see Figure 4 for complex **3a**) indicate that the electron transfer $\text{Ru}(\text{II}) \rightarrow \text{Ru}(\text{III})$ is reversible.⁷⁶ All of the 1,2-azolyamidino complexes described herein, as well as that of $[\text{Ru}(\text{bipy})_3]^{2+}$, present similar behavior (see the Supporting Information).⁷⁵

At negative potentials (0 to -1.8 V vs SCE) (see Figure S24 for **3b**), the electrochemistry of complexes **1**, **3**, and **4** is analogous to that of *cis*-bis(bipy)ruthenium(II) complexes and is associated with reduction processes centered at the bipyridine ligands.^{23,73,77–79} All of the 1,2-azolyamidino complexes described herein present similar behavior (see the Supporting Information).

From the ground-state redox potentials and the absorption and emission spectra of the Ru(II) complexes, we have

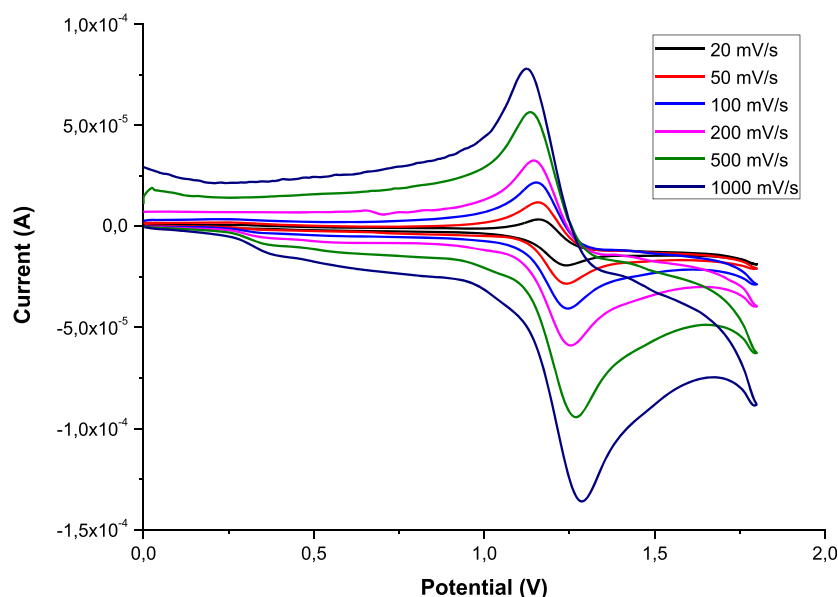
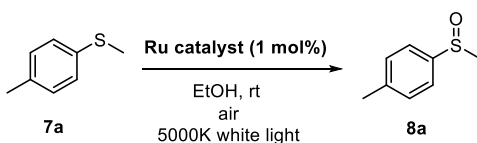


Figure 4. Cyclic voltammograms recorded in 2 mM acetonitrile solutions of 3a at different scan rates (from 20 to 1000 mV/s).

Table 5. Photooxidation of Sulfide 7a with 1,2-Azolyamidino Complexes 3 and 4^a



entry	catalyst	conversion (%) ^b		
		t = 15 min	t = 30 min	t = 60 min
1	[Ru(bipy) ₃] ²⁺	60	84	100
2	3a	13	18	30
3	3b	17	40	81
4	3c	89	92	100
5	4a	1	2	10
6	4b	1	6	10
7	4c	1	2	5
8	1b	0	0	0
9	1c	0	0	0
10	2b	0	0	0

^aReaction conditions: open vials containing 7a (0.2 mmol) and 1 mol % of the corresponding Ru(II) complex in 2 mL of EtOH were irradiated under white light for the indicated time. ^bDetermined by ¹H NMR analysis of the crude mixture.

estimated the excited-state redox potentials of the most catalytically active complexes 3a–c (see below), which are detailed in Table 4. The excited-state oxidation and reduction potentials values of these complexes were very similar to each other, regardless of the nature of the 1,2-azolyamidino ligand of complexes 3a–c.

Photocatalytic Studies. The photocatalytic activity of the 1,2-azolyamidino complexes was tested in the oxidation of sulfides as a model reaction, using ambient oxygen as the oxidant.^{26,28,80–87} The oxidations were performed using methyl *p*-tolyl sulfide 7a as sulfide and 1 mol % of the Ru(II) complex 3 or 4 in ethanol (Table 5). The reaction mixture was stirred open to the air under white-light irradiation. In addition, the complex [Ru(bipy)₃]²⁺, one of the most widely used photocatalysts, was also evaluated under the same conditions.

Using this complex, the oxidation of 7a was fully accomplished in only 1 h (entry 1). With regard to the 1,2-azolyamidino complexes, the catalytic activities of 3a–c (entries 2–4) were remarkably higher than those of s 4a–c (entries 5–7). These results highlight the importance of the phenyl group (R'; see Scheme 2) at the 1,2-azolyamidino ligand in the activity of the photocatalyst for this transformation. In addition, the best catalytic performance was obtained with catalyst 3c, which was able to oxidize 92% of sulfide 7a in only 30 min (entry 4). This activity is even higher than that of [Ru(bipy)₃]²⁺ (entry 1) under the same catalytic conditions. Finally, the catalytic performance of the precursors 1b,c and 2, as selected examples, was also evaluated (entries 8–10), these being totally inactive photocatalysts for this transformation.

The catalytic performance should be related to the physical properties of the catalyst. Therefore, the absorption and emission spectra, quantum yields, and lifetimes in MeOH and CD₃OD were measured for 3c, which showed the best catalytic performance. The results are collected in Figure S26 and Table S10 in the the Supporting Information. The spectra of 3c in MeOH and CD₃OD are very similar to those in MeCN, THF, and acetone (Figure S19), although the lifetime is reduced in methanol (131 ns for MeOH, 136 ns for CD₃OD) in comparison to THF (304 ns in THF). There are no significant differences between the data in MeOH and those in CD₃OD.

Next, the activity of catalyst 3c was studied using sulfides of different nature under the best reaction conditions (Scheme 3). Complex 3c was able to chemoselectively catalyze the oxidation of benzyl sulfide 7b and allyl sulfide 7c in high yields, without detection of any other byproduct from the oxidation of the benzylic position or the double bond. Dialkyl sulfides 7d,e were also easily oxidized, the corresponding sulfoxides being isolated in 75% and 78% yields, respectively. Conversely, the oxidation of methyl *p*-nitrophenyl sulfide (7g) did not take place, suggesting that the oxidation reaction goes through a photoredox mechanism, as explained below. Finally, the applicability of the catalytic system was evaluated in the preparation of the drug modafinil, which is a wake-promoting agent.⁸⁸ This drug (8f) was also successfully prepared in 79% yield in only 1 h using complex 3c as the photocatalyst, under

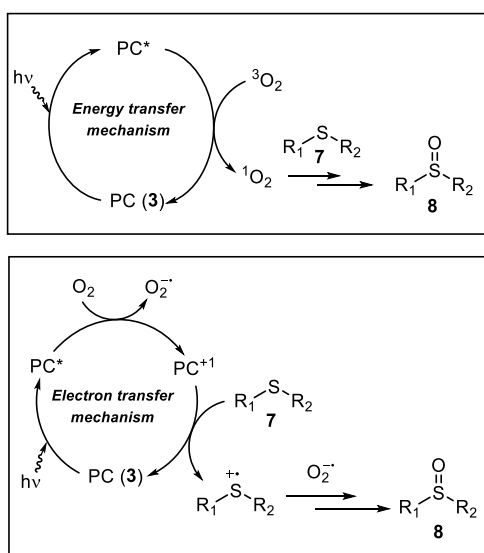
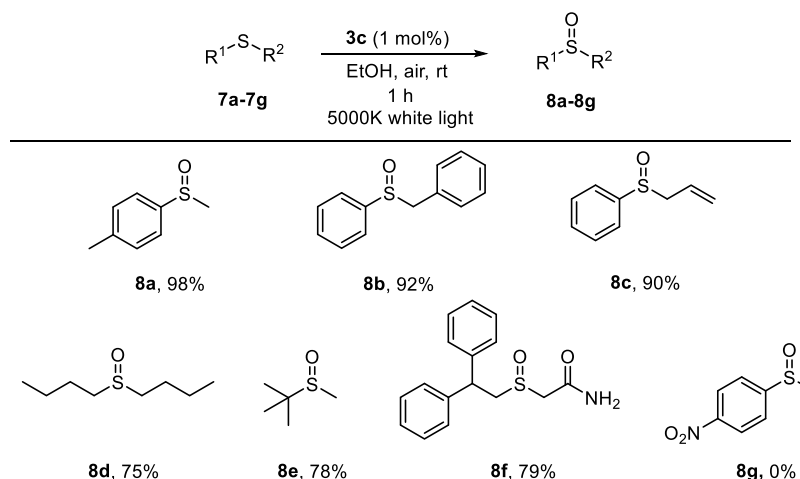
Scheme 3. Scope of the Photooxidation Reaction of Sulfides **7** using Catalyst **3c**

Figure 5. Two possible mechanistic pathways for the photooxidation of sulfides under visible-light irradiation.

environmentally friendly oxidation conditions. It is important to mention that the oxidation proceeds chemoselectively to the formation of the sulfoxide in all of the cases studied, overoxidation to the sulfone never being observed.

With regard to the mechanism, two different pathways are possible for the photooxidation of sulfides (Figure 5): (a) an energy transfer process, which produces singlet oxygen, or (b) a photoredox process, which involves superoxide radical anion and sulfide radical cation species.⁸¹ Distinguishing between both mechanisms is not easy, but the addition of selective quenchers or enhancers of the reactive oxygen species can help to identify the predominant pathway. These experiments were performed with methyl *p*-tolyl sulfide (**7a**) in MeOH as solvent, and the reaction was stopped after 10 min (Table 6). Parallel experiments were carried out using catalyst **3c** or [Ru(bipy)₃]²⁺, and analogous results were obtained in all of the experiments. It is known that the use of deuterated solvents accelerates oxidation reactions mediated by singlet oxygen.⁸² In our case, similar results were obtained when the reactions were performed using MeOH or CD₃OD (entries 1 and 2). Conversely, the addition of sodium azide as a scavenger of the singlet oxygen species completely inhibited the reaction (entry 3), pointing to an energy transfer process. On the other hand, the outcome of the oxidation of **7a** in the presence of a scavenger of the sulfide radical cation, such as 1,4-dimethoxybenzene, or a scavenger of the superoxide radical, such as benzoquinone, would indicate the contribution of the photoredox pathway.⁸¹ Moreover, while the presence of benzoquinone fully suppressed the oxidation process (entry 5), the addition of 1,4-dimethoxybenzene induced a slight decrease in the formation of **8a** (entry 4). An analogous

Table 6. Mechanistic Tests Using Scavengers or Enhancers

entry	solvent	additive (0.5 equiv)	aim	conversion (%) ^a	
				3c	[Ru(bipy) ₃] ²⁺
1	CH ₃ OH			60	58
2	CD ₃ OD		enhancing ¹ O ₂ -mediated pathway	65	62
3	CH ₃ OH	NaN ₃	¹ O ₂ scavenger	0	0
4	CH ₃ OH	1,4-dimethoxybenzene	R ₂ S ⁺ scavenger	53	57
5	CH ₃ OH	benzoquinone	O ₂ ^{-•} scavenger	0	0

^aConversion determined by an ¹H NMR analysis of the crude mixture.

mechanistic study with scavengers was carried out using catalysts **3a,b**, giving the same inhibition trends (Table S11). All of the mechanistic experiments, together with the unsuccessful oxidation of the *p*-nitro sulfide derivative **7f**, suggest the participation of radical intermediates in the mechanism. In summary, all of these mechanistic experiments point out that both energy transfer and photoredox processes are taking place in the photooxidation of sulfides using the 1,2-azoylamidino ruthenium complexes **3** as catalysts.

CONCLUSIONS

A new family of *cis*-Ru^{II}(bipy)₂ complexes with the 1,2-azoylamidino ligand has been synthesized and thoroughly characterized by ¹H, ¹³C, and ¹⁵N NMR and IR spectroscopy and single-crystal X-ray diffractometry. The complexes show phosphorescent emissions with quantum yields and lifetimes comparable to those of other analogous complexes. The redox properties are similar to those of [Ru(bipy)₃]²⁺, with reversible Ru^{II}/Ru^{III} oxidations between +1.13 and +1.25 V (vs SCE). Moreover, the 1,2-azoylamidino complexes can be used as catalysts in the photooxidation of different thioethers. In fact, the dimethylpyrazolyamidino complex *cis*-[Ru(bipy)₂(NH=C(Me)dmpz-κ²N,N)]²⁺, which presents the highest quantum yield and also the highest luminescent emission lifetime, shows a better catalytic performance in comparison to that of [Ru(bipy)₃]²⁺. Among the wide range of *cis*-Ru^{II}(bipy)₂ complexes reported, the family of 1,2-azoylamidino complexes described herein has the advantages of facile synthesis and the ability to fine-tune the electrochemical, luminescent, and catalytic activity by varying the steric and electronic effects of the 1,2-azole and nitrile precursors.

ASSOCIATED CONTENT

Supporting Information

The Supporting Information is available free of charge at <https://pubs.acs.org/doi/10.1021/acs.inorgchem.0c03389>.

Additional characterization and experimental data and crystal structures of complexes **3a–c** and **4a–c** (PDF)

Accession Codes

CCDC 2044577–2044582 contain the supplementary crystallographic data for this paper. These data can be obtained free of charge via www.ccdc.cam.ac.uk/data_request/cif, or by emailing data_request@ccdc.cam.ac.uk, or by contacting The Cambridge Crystallographic Data Centre, 12 Union Road, Cambridge CB2 1EZ, UK; fax: +44 1223 336033.

AUTHOR INFORMATION

Corresponding Author

Fernando Villafañe – GIR MIOMeT-IU Cincuenta-Química Inorgánica, Facultad de Ciencias, Campus Miguel Delibes, Universidad de Valladolid, 47011 Valladolid, Spain; orcid.org/0000-0002-3230-3802; Email: fernando.villafane@uva.es

Authors

Elena Cuéllar – GIR MIOMeT-IU Cincuenta-Química Inorgánica, Facultad de Ciencias, Campus Miguel Delibes, Universidad de Valladolid, 47011 Valladolid, Spain
Alberto Díez-Varga – Departamento de Química, Facultad de Ciencias, Universidad de Burgos, 09001 Burgos, Spain

Tomás Torroba – Departamento de Química, Facultad de Ciencias, Universidad de Burgos, 09001 Burgos, Spain; orcid.org/0000-0002-5018-4173

Pablo Domingo-Legarda – Departamento de Química Inorgánica, Facultad de Ciencias, Universidad Autónoma de Madrid, 28049 Madrid, Spain

José Alemán – Departamento de Química Inorgánica, Facultad de Ciencias, Universidad Autónoma de Madrid, 28049 Madrid, Spain; orcid.org/0000-0003-0164-1777

Silvia Cabrera – Departamento de Química Inorgánica, Facultad de Ciencias, Universidad Autónoma de Madrid, 28049 Madrid, Spain; orcid.org/0000-0002-4907-2932

Jose M. Martín-Alvarez – GIR MIOMeT-IU Cincuenta-Química Inorgánica, Facultad de Ciencias, Campus Miguel Delibes, Universidad de Valladolid, 47011 Valladolid, Spain; orcid.org/0000-0002-6969-0703

Daniel Miguel – GIR MIOMeT-IU Cincuenta-Química Inorgánica, Facultad de Ciencias, Campus Miguel Delibes, Universidad de Valladolid, 47011 Valladolid, Spain; orcid.org/0000-0003-0650-3058

Complete contact information is available at: <https://pubs.acs.org/doi/10.1021/acs.inorgchem.0c03389>

Author Contributions

The manuscript was written through contributions of all authors. All authors have given approval to the final version of the manuscript.

Notes

The authors declare no competing financial interest.

ACKNOWLEDGMENTS

The authors in Valladolid gratefully acknowledge financial support from the Spanish MINECO of Spain (PGC2018-099470-B-I00) and Junta de Castilla y León (VA130618), and the authors in Burgos gratefully acknowledge financial support from the Junta de Castilla y León, Consejería de Educación y Cultura y Fondo Social Europeo (Project BU263P18). E.C. thanks the UVa for her grant. The authors in Universidad Autónoma de Madrid acknowledge financial support from the Spanish MINECO (RTI2018-095038-B-I00). We also thank Gabriel García-Herbosa and Irene Abajo-Cuadrado (Universidad de Burgos, Burgos, Spain) for helping us with the electrochemical and photophysical experiments, respectively.

REFERENCES

- Paris, J. P.; Brandt, W. W. Charge Transfer Luminescence of A Ruthenium(II) Chelate. *J. Am. Chem. Soc.* **1959**, *81* (18), 5001–5002.
- Creutz, C.; Taube, H. Direct Approach to Measuring the Franck-Condon Barrier to Electron Transfer between Metal Ions. *J. Am. Chem. Soc.* **1969**, *91* (14), 3988–3989.
- Vos, J. G.; Kelly, J. M. Ruthenium Polypyridyl Chemistry; from Basic Research to Applications and Back Again. *Dalton Trans.* **2006**, *41*, 4869–4883.
- Zhou, J.; Liu, Q.; Feng, W.; Sun, Y.; Li, F. Upconversion Luminescent Materials: Advances and Applications. *Chem. Rev.* **2015**, *115* (1), 395–465.
- Morris, A. J.; Meyer, G. J.; Fujita, E. Molecular Approaches to the Photocatalytic Reduction of Carbon Dioxide for Solar Fuels. *Acc. Chem. Res.* **2009**, *42* (12), 1983–1994.
- Bléger, D.; Hecht, S. Visible-Light-Activated Molecular Switches. *Angew. Chem., Int. Ed.* **2015**, *54* (39), 11338–11349.
- Yeung, M. C.-L.; Yam, V. W.-W. Luminescent Cation Sensors: From Host-Guest Chemistry, Supramolecular Chemistry to Reaction-Based Mechanisms. *Chem. Soc. Rev.* **2015**, *44* (13), 4192–4202.

- (8) Erkkila, K. E.; Odom, D. T.; Barton, J. K. Recognition and Reaction of Metallointercalators with DNA. *Chem. Rev.* **1999**, *99* (9), 2777–2796.
- (9) Lo, K. K. W.; Hui, W. K.; Chung, C. K.; Tsang, K. H. K.; Lee, T. K. M.; Li, C. K.; Lau, J. S. Y.; Ng, D. C. M. Luminescent Transition Metal Complex Biotin Conjugates. *Coord. Chem. Rev.* **2006**, *250* (13–14), 1724–1736.
- (10) Lo, K. K. W.; Tsang, K. H. K.; Sze, K. S.; Chung, C. K.; Lee, T. K. M.; Zhang, K. Y.; Hui, W. K.; Li, C. K.; Lau, J. S. Y.; Ng, D. C. M. Non-Covalent Binding of Luminescent Transition Metal Polypyridine Complexes to Avidin, Indole-Binding Proteins and Estrogen Receptors. *Coord. Chem. Rev.* **2007**, *251* (17–20), 2292–2310.
- (11) Fernández-Moreira, V.; Thorp-Greenwood, F. L.; Coogan, M. P. Application of D6 Transition Metal Complexes in Fluorescence Cell Imaging. *Chem. Commun.* **2010**, *46* (2), 186–202.
- (12) Zhao, Q.; Huang, C.; Li, F. Phosphorescent Heavy-Metal Complexes for Bioimaging. *Chem. Soc. Rev.* **2011**, *40* (5), 2508.
- (13) Smith, J. A.; George, M. W.; Kelly, J. M. Transient Spectroscopy of Dipyrrophenazine Metal Complexes Which Undergo Photo-Induced Electron Transfer with DNA. *Coord. Chem. Rev.* **2011**, *255* (21–22), 2666–2675.
- (14) Baggaley, E.; Weinstein, J. A.; Williams, J. A. G. Lighting the Way to See inside the Live Cell with Luminescent Transition Metal Complexes. *Coord. Chem. Rev.* **2012**, *256* (15–16), 1762–1785.
- (15) Lo, K. K.-W.; Choi, A. W.-T.; Law, W. H.-T. Applications of Luminescent Inorganic and Organometallic Transition Metal Complexes as Biomolecular and Cellular Probes. *Dalton Trans.* **2012**, *41* (20), 6021–6047.
- (16) Ma, D. L.; He, H. Z.; Leung, K. H.; Chan, D. S. H.; Leung, C. H. Bioactive Luminescent Transition-Metal Complexes for Biomedical Applications. *Angew. Chem., Int. Ed.* **2013**, *52* (30), 7666–7682.
- (17) Marcéls, L.; Ghesquière, J.; Garnir, K.; Kirsch-De Mesmaeker, A.; Moucheron, C. Photo-Oxidizing RuII complexes and Light: Targeting Biomolecules via Photoadditions. *Coord. Chem. Rev.* **2012**, *256* (15–16), 1569–1582.
- (18) Prier, C. K.; Rankic, D. A.; MacMillan, D. W. C. Visible Light Photoredox Catalysis with Transition Metal Complexes: Applications in Organic Synthesis. *Chem. Rev.* **2013**, *113* (7), 5322–5363.
- (19) Uygur, M.; García Mancheño, O. Visible Light-Mediated Organophotocatalyzed C-H Bond Functionalization Reactions. *Org. Biomol. Chem.* **2019**, *17* (22), 5475–5489.
- (20) Jang, H. J.; Hopkins, S. L.; Siegler, M. A.; Bonnet, S. Frontier Orbitals of Photosubstitutionally Active Ruthenium Complexes: An Experimental Study of the Spectator Ligands' Electronic Properties Influence on Photoreactivity. *Dalton Trans.* **2017**, *46* (30), 9969–9980.
- (21) Angerani, S.; Winssinger, N. Visible Light Photoredox Catalysis Using Ruthenium Complexes in Chemical Biology. *Chem. - Eur. J.* **2019**, *25* (27), 6661–6672.
- (22) Narayanam, J. M. R.; Stephenson, C. R. J. Visible Light Photoredox Catalysis: Applications in Organic Synthesis. *Chem. Soc. Rev.* **2011**, *40* (1), 102–113.
- (23) Juris, A.; Balzani, V.; Barigelli, F.; Campagna, S.; Belser, P.; von Zelewsky, A. Ru(II) Polypyridine Complexes: Photophysics, Photochemistry, Electrochemistry, and Chemiluminescence. *Coord. Chem. Rev.* **1988**, *84*, 85–277.
- (24) Kalyanasundaram, K. Photophysics, Photochemistry and Solar Energy Conversion with Tris(Bipyridyl)Ruthenium(II) and Its Analogues. *Coord. Chem. Rev.* **1982**, *46*, 159–244.
- (25) Juris, A.; Balzani, V.; Belser, P.; von Zelewsky, A. Characterization of the Excited State Properties of Some New Photosensitizers of the Ruthenium (Polypyridine) Family. *Helv. Chim. Acta* **1981**, *64* (7), 2175–2182.
- (26) Casado-Sánchez, A.; Gómez-Ballesteros, R.; Tato, F.; Soriano, F. J.; Pascual-Coca, G.; Cabrera, S.; Alemán, J. Pt(II) Coordination Complexes as Visible Light Photocatalysts for the Oxidation of Sulfides Using Batch and Flow Processes. *Chem. Commun.* **2016**, *52* (58), 9137–9140.
- (27) Hikita, T.; Tamaru, K.; Yamagishi, A.; Iwamoto, T. Production of an Optically Active Sulfoxide by Use of Colloidally Dispersed Tris(2,2'-Bipyridyl)Ruthenium(II) Montmorillonite as a Photosensitizer. *Inorg. Chem.* **1989**, *28* (11), 2221–2223.
- (28) Zen, J.-M.; Liou, S.-L.; Kumar, A. S.; Hsia, M.-S. An Efficient and Selective Photocatalytic System for the Oxidation of Sulfides to Sulfoxides. *Angew. Chem., Int. Ed.* **2003**, *42* (5), 577–579.
- (29) Fujita, S.; Sato, H.; Kakegawa, N.; Yamagishi, A. Enantioselective Photooxidation of a Sulfide by a Chiral Ruthenium(II) Complex Immobilized on a Montmorillonite Clay Surface: The Role of Weak Interactions in Asymmetric Induction. *J. Phys. Chem. B* **2006**, *110* (6), 2533–2540.
- (30) Li, T.-T.; Shan, B.; Xu, W.; Meyer, T. J. Electrocatalytic CO₂ Reduction with a Ruthenium Catalyst in Solution and on Nanocrystalline TiO₂. *ChemSusChem* **2019**, *12*, 1–8.
- (31) Garrido-Barros, P.; Funes-Ardoiz, I.; Farràs, P.; Gimbert-Suriñach, C.; Maseras, F.; Llobet, F. A. 2.3 Water as an Oxygen Source for Oxidation Reactions. In *Catalytic Oxidation in Organic Synthesis*; Muñiz, K., Ed.; Georg Thieme Verlag: Stuttgart, Germany, 2018.
- (32) Farràs, P.; Di Giovanni, C.; Clifford, J. N.; Palomares, E.; Llobet, A. H₂ Generation and Sulfide to Sulfoxide Oxidation with H₂O and Sunlight with a Model Photoelectrosynthesis Cell. *Coord. Chem. Rev.* **2015**, *304–305*, 202–208.
- (33) Riley, D. P.; Oliver, J. D. Ruthenium(II)-Catalyzed Thioether Oxidation. 1. Synthesis of Mixed Sulfide and Sulfoxide Complexes. *Inorg. Chem.* **1986**, *25* (11), 1814–1821.
- (34) Carreño, M. C.; Hernández-Torres, G.; Ribagorda, M.; Urbano, A. Enantiopure Sulfoxides: Recent Applications in Asymmetric Synthesis. *Chem. Commun.* **2009**, *7345* (41), 6129–6144.
- (35) Feng, M.; Tang, B. H.; Liang, S.; Jiang, X. Sulfur Containing Scaffolds in Drugs: Synthesis and Application in Medicinal Chemistry. *Curr. Top. Med. Chem.* **2016**, *16* (11), 1200–1216.
- (36) Hage, R.; Prins, R.; Haasnoot, J. G.; Reedijk, J.; Vos, J. G. Synthesis, Spectroscopic, and Electrochemical Properties of Bis(2,2'-Bipyridyl)-Ruthenium Compounds of Some Pyridyl-1,2,4-Triazoles. *J. Chem. Soc., Dalton Trans.* **1987**, *6*, 1389–1395.
- (37) Steel, P. J.; Constable, E. C. Synthesis, Spectroscopy, and Electrochemistry of Homo- and Hetero-Leptic Ruthenium(II) Complexes of New Pyrazole-Containing Bidentate Ligands. *J. Chem. Soc., Dalton Trans.* **1990**, *4*, 1389–1396.
- (38) Gómez-Iglesias, P.; Arroyo, M.; Bajo, S.; Strohmman, C.; Miguel, D.; Villafañe, F. Pyrazolylamidino Ligands from Coupling of Acetonitrile and Pyrazoles: A Systematic Study. *Inorg. Chem.* **2014**, *53* (23), 12437–12448.
- (39) Cuéllar, E.; Pastor, L.; García-Herbosa, G.; Nganga, J.; Angeles-Boza, A. M.; Diez-Varga, A.; Torroba, T.; Martín-Alvarez, J. M.; Miguel, D.; Villafañe, F. (1,2-Azole)Bis(Bipyridyl)Ruthenium(II) Complexes: Electrochemistry, Luminescent Properties, and Electro-And Photocatalysts for CO₂ Reduction. *Inorg. Chem.* **2021**, *60* (2), 692–704.
- (40) Jiménez-Almarza, A.; López-Magano, A.; Marzo, L.; Cabrera, S.; Mas-Ballesté, R.; Alemán, J. Imine-Based Covalent Organic Frameworks as Photocatalysts for Metal Free Oxidation Processes under Visible Light Conditions. *ChemCatChem* **2019**, *11* (19), 4916–4922.
- (41) Dolomanov, O. V.; Bourhis, L. J.; Gildea, R. J.; Howard, J. A. K.; Puschmann, H. OLEX2: A Complete Structure Solution, Refinement and Analysis Program. *J. Appl. Crystallogr.* **2009**, *42* (2), 339–341.
- (42) Sheldrick, G. M. Crystal Structure Refinement with SHELXL. *Acta Crystallogr., Sect. C: Struct. Chem.* **2015**, *71* (Md), 3–8.
- (43) Sheldrick, G. M. A Short History of SHELX. *Acta Crystallogr., Sect. A: Found. Crystallogr.* **2008**, *64* (1), 112–122.
- (44) Nardelli, M. Parst: A System of Fortran Routines for Calculating Molecular Structure Parameters from Results of Crystal Structure Analyses. *Comput. Chem.* **1983**, *7*, 95–98.
- (45) Nardelli, M. PARST 95 - an Update to PARST: A System of Fortran Routines for Calculating Molecular Structure Parameters

from the Results of Crystal Structure Analyses. *J. Appl. Crystallogr.* **1995**, *28* (5), 659–659.

(46) Jeffrey, G. A.; Lewis, L. Cooperative Aspects of Hydrogen Bonding in Carbohydrates. *Carbohydr. Res.* **1978**, *60* (1), 179–182.

(47) Taylor, R.; Kennard, O. Comparison of X-ray and Neutron Diffraction Results for the N-H...O = C Hydrogen Bond. *Acta Crystallogr., Sect. B: Struct. Sci.* **1983**, *39* (1), 133–138.

(48) Kollipara, M. R.; Sarkhel, P.; Chakraborty, S.; Lalrempuia, R. Synthesis, Characterization and Molecular Structure of a New (η^6 -p-Cymene) Ruthenium(II) Amidine Complex, $[(\eta^6$ -p-Cymene)Ru{NH = C(Me)₃,S-Dmpz}(3,5-Hdmpz)](BF₄)₂·H₂O. *J. Coord. Chem.* **2003**, *56* (12), 1085–1091.

(49) López, J.; Santos, A.; Romero, A.; Echavarren, A. M. Synthesis of Ru^{II} Hydride and Alkenyl Amidine Complexes. The Crystal Structure of [Ru(CO)(CH = CHCMe₃){NH = C(Me)(Me₂Pz)}-(PPh₃)₂][PF₆]. *J. Organomet. Chem.* **1993**, *443* (2), 221–228.

(50) Romero, A.; Vegas, A.; Santos, A. Reaction of [Ru(CO)H(NCMe)₂(PPh₃)₂][ClO₄] with 1-Hydroxymethyl-3,5-Dimethylpyrazole. Formation of an Amidine Complex. The Crystal Structure of [Ru(CO)H{NHCMe(Me₂Pz)}(PPh₃)₂][ClO₄]. *J. Organomet. Chem.* **1986**, *310* (1), C8–C10.

(51) Jones, C. J.; McCleverty, J. A.; Rothin, A. S. Reactions of Benzene-Ruthenium(II) Complexes with Pyrazoles. Possible Formation of Amidine Complexes [Ru(η -C₆H₆){NHCMe(R₂Pz)}-(R₂Hpz)]²⁺ (R = H or Me, Hpz = Pyrazole). *J. Chem. Soc., Dalton Trans.* **1986**, No. 1, 109–111.

(52) Govindaswamy, P.; Mozharivskiy, Y. A.; Kollipara, M. R. Reactivity Studies of (H₆-Arene)Ruthenium Dimeric Complexes towards Pyrazoles: Isolation of Amidines, Bis Pyrazoles and Chloro Bridged Pyrazole Complexes. *J. Organomet. Chem.* **2004**, *689* (20), 3265–3274.

(53) Jeffrey, A. G. *An Introduction to Hydrogen Bonding*; Oxford University Press: New York, 1997.

(54) Steiner, T. The Hydrogen Bond in the Solid State. *Angew. Chem., Int. Ed.* **2002**, *41* (1), 48–76.

(55) Richardson, C.; Steel, P. J. Di(2-Pyridyl)Furoxan: Metal Complexes and an Unusual Ruthenium-Induced Molecular Rearrangement. *Aust. J. Chem.* **2000**, *53* (2), 93–97.

(56) Ishida, H.; Tobita, S.; Hasegawa, Y.; Katoh, R.; Nozaki, K. Recent Advances in Instrumentation for Absolute Emission Quantum Yield Measurements. *Coord. Chem. Rev.* **2010**, *254* (21–22), 2449–2458.

(57) Steel, P. J.; LaHousse, F.; Lerner, D.; Marzin, C. New Ruthenium(II) Complexes with Pyridylpyrazole Ligands. Photo-substitution and Proton, Carbon-13, and Ruthenium-99 NMR Structural Studies. *Inorg. Chem.* **1983**, *22* (10), 1488–1493.

(58) Kajouj, S.; Marcélis, L.; Lemaire, V.; Beljonne, D.; Moucheron, C. Photochemistry of Ruthenium(II) Complexes Based on 1,4,5,8-Tetraazaphenanthrene and 2,2'-Bipyrazine: A Comprehensive Experimental and Theoretical Study. *Dalton Trans.* **2017**, *46* (20), 6623–6633.

(59) Whittemore, T. J.; White, T. A.; Turro, C. New Ligand Design Provides Delocalization and Promotes Strong Absorption throughout the Visible Region in a Ru(II) Complex. *J. Am. Chem. Soc.* **2018**, *140* (1), 229–234.

(60) Scalambra, F.; Serrano-Ruiz, M.; Nahim-Granados, S.; Romero, A. Ruthenium Complexes Containing 2,2'-Bipyridine and 1,3,5-Triaza-7-Phosphaadamantane. *Eur. J. Inorg. Chem.* **2016**, *2016* (10), 1528–1540.

(61) Galletta, M.; Campagna, S.; Quesada, M.; Ulrich, G.; Zissel, R. The Elusive Phosphorescence of Pyromethene-BF₂ Dyes Revealed in New Multicomponent Species Containing Ru(II)-Terpyridine Subunits. *Chem. Commun.* **2005**, No. 33, 4222.

(62) Müller, A. V.; Polo, A. S. Mechanistic Insights into the Stepwise Assembly of Ruthenium(II) Tris-Heteroleptic Compounds. *Inorg. Chem.* **2018**, *57* (21), 13829–13839.

(63) Wei, Q.-H.; Lei, Y.-F.; Duan, Y.-N.; Xiao, F.-N.; Li, M.-J.; Chen, G.-N. Mono- and Dinuclear Ru(II) Complexes of 1,4-Bis(3-(2-Pyridyl)Pyrazol-1-Ylmethyl)Benzene): Synthesis, Structure, Photo-

physical Properties and Electrochemiluminescent Determination of Diuretic Furosemide. *Dalton Trans.* **2011**, *40* (43), 11636.

(64) Chou, C.-C.; Hu, F.-C.; Wu, K.-L.; Duan, T.; Chi, Y.; Liu, S.-H.; Lee, G.-H.; Chou, P.-T. 4,4',5,5'-Tetracarboxy-2,2'-Bipyridine Ru(II) Sensitizers for Dye-Sensitized Solar Cells. *Inorg. Chem.* **2014**, *53* (16), 8593–8599.

(65) Valeur, B. Molecular Fluorescence. In *Digital Encyclopedia of Applied Physics*; Wiley-VCH: Weinheim, Germany, 2009; pp 477–531.

(66) Baba, H.; Goodman, L.; Valenti, P. C. Solvent Effects on the Fluorescence Spectra of Diazines. Dipole Moments in the (π, π^*) Excited States. *J. Am. Chem. Soc.* **1966**, *88* (23), 5410–5415.

(67) Gómez-Iglesias, P.; Guyon, F.; Khatyr, A.; Ulrich, G.; Knorr, M.; Martín-Alvarez, J. M.; Miguel, D.; Villafañe, F. Luminescent Rhenium(I) Tricarbonyl Complexes with Pyrazolylamidino Ligands: Photophysical, Electrochemical, and Computational Studies. *Dalton Trans.* **2015**, *44* (40), 17516–17528.

(68) Arroyo, M.; Miguel, D.; Villafañe, F.; Nieto, S.; Pérez, J.; Riera, L. Rhenium-Mediated Coupling of Acetonitrile and Pyrazoles. New Molecular Clefs for Anion Binding. *Inorg. Chem.* **2006**, *45* (17), 7018–7026.

(69) Catalan, J.; Claramunt, R. M.; Elguero, J.; Laynez, J.; Menendez, M.; Anvia, F.; Quian, J. H.; Taagepera, M.; Taft, R. W. Basicity and Acidity of Azoles: The Annulation Effect in Azoles. *J. Am. Chem. Soc.* **1988**, *110* (13), 4105–4111.

(70) Elguero, J.; Yranzo, G. I.; Laynez, J.; Jimenez, P.; Menendez, M.; Catalan, J.; De Paz, J. L. G.; Anvia, F.; Taft, R. W. Effect of the Replacement of a Methyl by a Trifluoromethyl Group on the Acid-Base Properties of Pyrazoles. *J. Org. Chem.* **1991**, *56* (12), 3942–3947.

(71) Anderson, P. A.; Deacon, G. B.; Haarmann, K. H.; Keene, F. R.; Meyer, T. J.; Reitsma, D. A.; Skelton, B. W.; Strouse, G. F.; Thomas, N. C. Designed Synthesis of Mononuclear Tris(Heteroleptic) Ruthenium Complexes Containing Bidentate Polypyridyl Ligands. *Inorg. Chem.* **1995**, *34* (24), 6145–6157.

(72) Nakamaru, K. Solvent Effect on the Nonradiative Deactivation of the Excited State of Tris(2,2'-Bipyridyl)Ruthenium(II) Ion. *Bull. Chem. Soc. Jpn.* **1982**, *55* (5), 1639–1640.

(73) Sá, D. S.; Fernandes, A. F.; Silva, C. D. S.; Costa, P. P. C.; Fonteles, M. C.; Nascimento, N. R. F.; Lopes, L. G. F.; Sousa, E. H. S. Non-Nitric Oxide Based Metallovasodilators: Synthesis, Reactivity and Biological Studies. *Dalton Trans.* **2015**, *44* (30), 13633–13640.

(74) Jude, H.; Rein, F. N.; Chen, W.; Scott, B. L.; Dattelbaum, D. M.; Rocha, R. C. Pyrazole and Pyrazolyl Complexes of Cis-Bis(2,2'-Bipyridine)-Chlororuthenium(II): Synthesis, Structural and Electronic Characterization, and Acid-Base Chemistry. *Eur. J. Inorg. Chem.* **2009**, *2009*, 683–690.

(75) Bock, C. R.; Connor, J. A.; Gutierrez, A. R.; Meyer, T. J.; Whitten, D. G.; Sullivan, B. P.; Nagle, J. K. Estimation of Excited-State Redox Potentials by Electron-Transfer Quenching. Application of Electron-Transfer Theory to Excited-State Redox Processes. *J. Am. Chem. Soc.* **1979**, *101* (17), 4815–4824.

(76) Heinze, J. Cyclic Voltammetry—“Electrochemical Spectroscopy”. *New Analytical Methods* (25). *Angew. Chem., Int. Ed. Engl.* **1984**, *23* (11), 831–847.

(77) Cruz, A. J.; Kirgan, S.; Siam, K.; Heiland, P.; Rillema, D. P. Photochemical and Photophysical Properties of Ruthenium(II) Bis-Bipyridine Bis-Nitrile Complexes: Photolability. *Inorg. Chim. Acta* **2010**, *363* (11), 2496–2505.

(78) Sullivan, B. P.; Conrad, D.; Meyer, T. J. Chemistry of Highly Reduced Polypyridyl-Metal Complexes. Anion Substitution Induced by Ligand-Based Reduction. *Inorg. Chem.* **1985**, *24* (22), 3640–3645.

(79) Ngo, K. T.; Lee, N. A.; Pinnace, S. D.; Szalda, D. J.; Weber, R. T.; Rochford, J. Probing the Noninnocent π -Bonding Influence of N-Carboxyamidoquinolate Ligands on the Light Harvesting and Redox Properties of Ruthenium Polypyridyl Complexes. *Inorg. Chem.* **2016**, *55* (5), 2460–2472.

(80) Vaquero, M.; Ruiz-Riaguas, A.; Martínez-Alonso, M.; Jalón, F. A.; Manzano, B. R.; Rodríguez, A. M.; García-Herbosa, G.; Carbayo,

A.; García, B.; Espino, G. Selective Photooxidation of Sulfides Catalyzed by Bis-Cyclometalated Ir^{III} Photosensitizers Bearing 2,2'-Dipyridylamine-Based Ligands. *Chem. - Eur. J.* **2018**, *24* (42), 10662–10671.

(81) Bonesi, S. M.; Manet, I.; Freccero, M.; Fagnoni, M.; Albini, A. Photosensitized Oxidation of Sulfides: Discriminating between the Singlet-Oxygen Mechanism and Electron Transfer Involving Superoxide Anion or Molecular Oxygen. *Chem. - Eur. J.* **2006**, *12* (18), 4844–4857.

(82) Dad'ová, J.; Svobodová, E.; Sikorski, M.; König, B.; Cibulka, R. Photooxidation of Sulfides to Sulfoxides Mediated by Tetra-O-Acetylriboflavin and Visible Light. *ChemCatChem* **2012**, *4* (5), 620–623.

(83) Gu, X.; Li, X.; Chai, Y.; Yang, Q.; Li, P.; Yao, Y. A Simple Metal-Free Catalytic Sulfoxidation under Visible Light and Air. *Green Chem.* **2013**, *15* (2), 357.

(84) Wang, H.; Wagner, G. W.; Lu, A. X.; Nguyen, D. L.; Buchanan, J. H.; McNutt, P. M.; Karwacki, C. J. Photocatalytic Oxidation of Sulfur Mustard and Its Simulant on BODIPY-Incorporated Polymer Coatings and Fabrics. *ACS Appl. Mater. Interfaces* **2018**, *10* (22), 18771–18777.

(85) Wei, H.; Guo, Z.; Liang, X.; Chen, P.; Liu, H.; Xing, H. Selective Photooxidation of Amines and Sulfides Triggered by a Superoxide Radical Using a Novel Visible-Light-Responsive Metal-Organic Framework. *ACS Appl. Mater. Interfaces* **2019**, *11* (3), 3016–3023.

(86) Guo, H.; Xia, H.; Ma, X.; Chen, K.; Dang, C.; Zhao, J.; Dick, B. Efficient Photooxidation of Sulfides with Amidated Alloxazines as Heavy-Atom-Free Photosensitizers. *ACS Omega* **2020**, *5* (18), 10586–10595.

(87) López-Magano, A.; Platero-Prats, A. E.; Cabrera, S.; Mas-Ballesté, R.; Alemán, J. Incorporation of Photocatalytic Pt(II) Complexes into Imine-Based Layered Covalent Organic Frameworks (COFs) through Monomer Truncation Strategy. *Appl. Catal., B* **2020**, *272*, 119027.

(88) Murillo-Rodríguez, E.; Barciela Veras, A.; Barbosa Rocha, N.; Budde, H.; Machado, S. An Overview of the Clinical Uses, Pharmacology, and Safety of Modafinil. *ACS Chem. Neurosci.* **2018**, *9* (2), 151–158.